

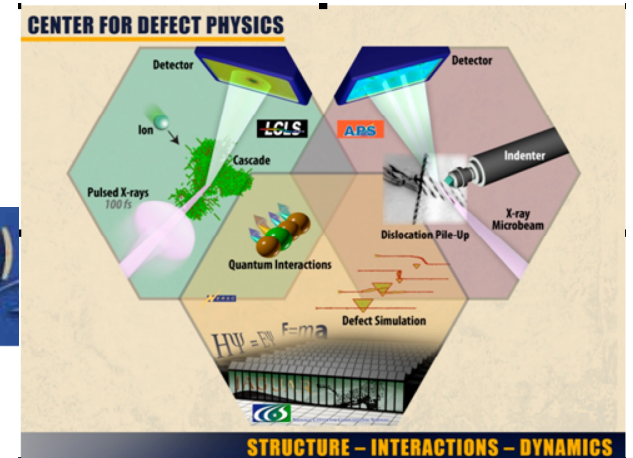
X-Ray Scattering Investigations of Defects in Crystalline Materials

Ben Larson

Materials Science and Technology Division
Oak Ridge National Laboratory
Oak Ridge, TN 37831

Center for Materials Science
of Nuclear Fuel

CENTER FOR DEFECT PHYSICS (CDP)
an Energy Frontier Research Center



Joint EFRC Summer School
Idaho Falls, ID; June 8, 2011

Research supported by the US Department of Energy, Office of Basic Energy Sciences as part of an Energy Frontier Research Center

Overview

- Perspective on scattering for investigating radiation defects
- Scattering response of crystals with lattice defects
- Diffuse scattering theory for lattice defects
- Diffuse scattering for investigating precipitates and radiation induced loops
- Techniques for investigating displacement cascade dynamics on time scales from milliseconds to picoseconds

Comments and Perspective

- The presentation emphasizes x-ray scattering, although the concepts discussed apply to neutron and electron scattering as well
 - Electron microscopy provides direct imaging of clustered defects, which is of course the measurement of choice for electrons
 - Neutron small angle diffuse scattering has been particularly useful in studies of clustered defects such as voids and precipitates
 - Neutrons are often more valuable for investigations that x-rays are not able to address well (e.g. magnetism, hydrogenous materials, etc.)
- *The lecture is meant to be used in conjunction with the below referenced book chapter review and references therein, **

*B. C. Larson, "X-ray Diffuse Scattering Near Bragg Reflections For The Study Of Clustered Defects In Crystalline Materials," in *Diffuse Scattering and the Fundamental Properties of Materials*, ed. Barabash, Ice, & Turchi (Momentum Press, New York, NY 2009). [pdf copy provided]

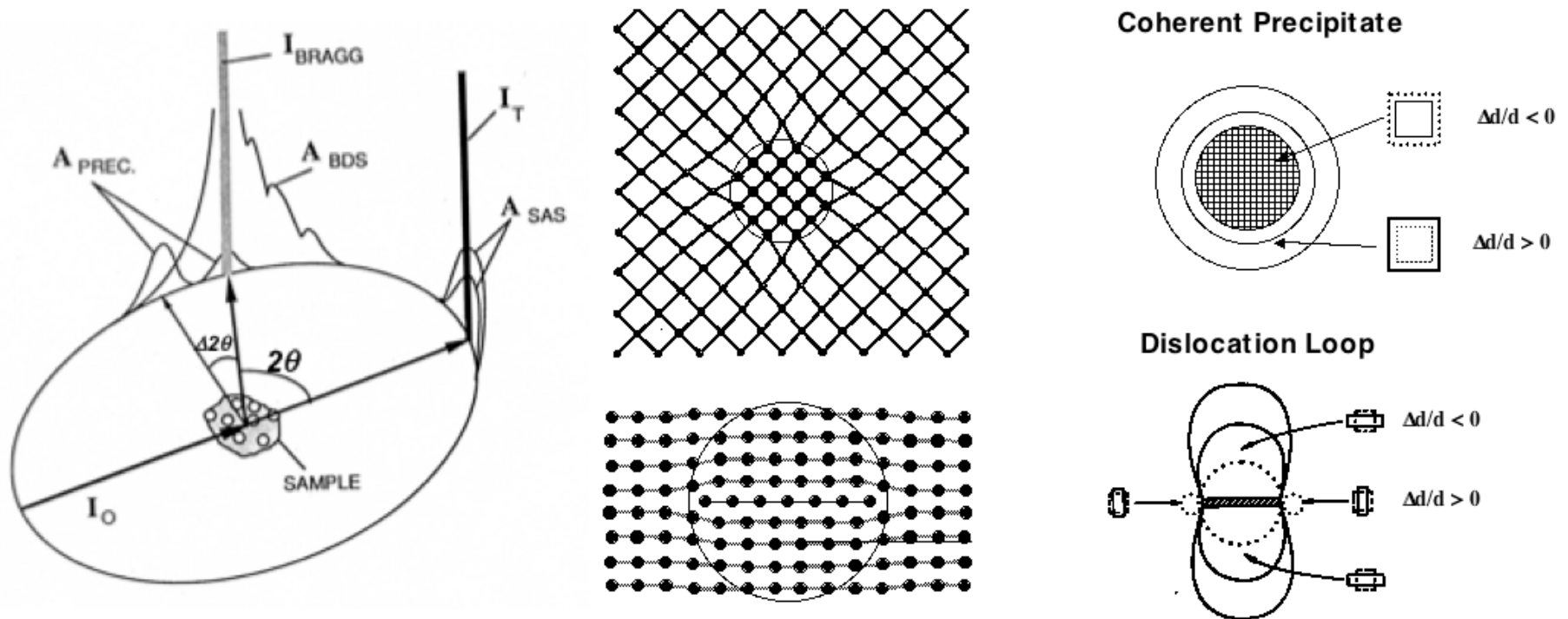
(Cont.)

Comments and Perspective (cont.)

- Radiation induced defects have important timescales from sub-picooseconds to giga-seconds (~40 years – reactor lifetimes) – **20 orders of magnitude**
- Damage includes dislocation loops, voids, dislocation tangles, radiation enhanced precipitates, as well as grain-boundary impacted/denuded zones and other local microstructure effects.
- For **ensembles of point defect clusters and microstructural complexities** there is **no substitute for the direct imaging** electron microscopy capabilities
- There is a **tradeoff between direct observation** on the one hand versus **non-destructive measurements, small cluster visibility, sequential annealing experiments, and in-situ measurements** on the other
- **The employment of multiple measurement types and close connections with theory and modeling is of almost indispensable value**
- The interpretation of picosecond time-resolved diffuse scattering from displacement cascades is an example in which molecular dynamics based diffuse scattering simulations will be critical

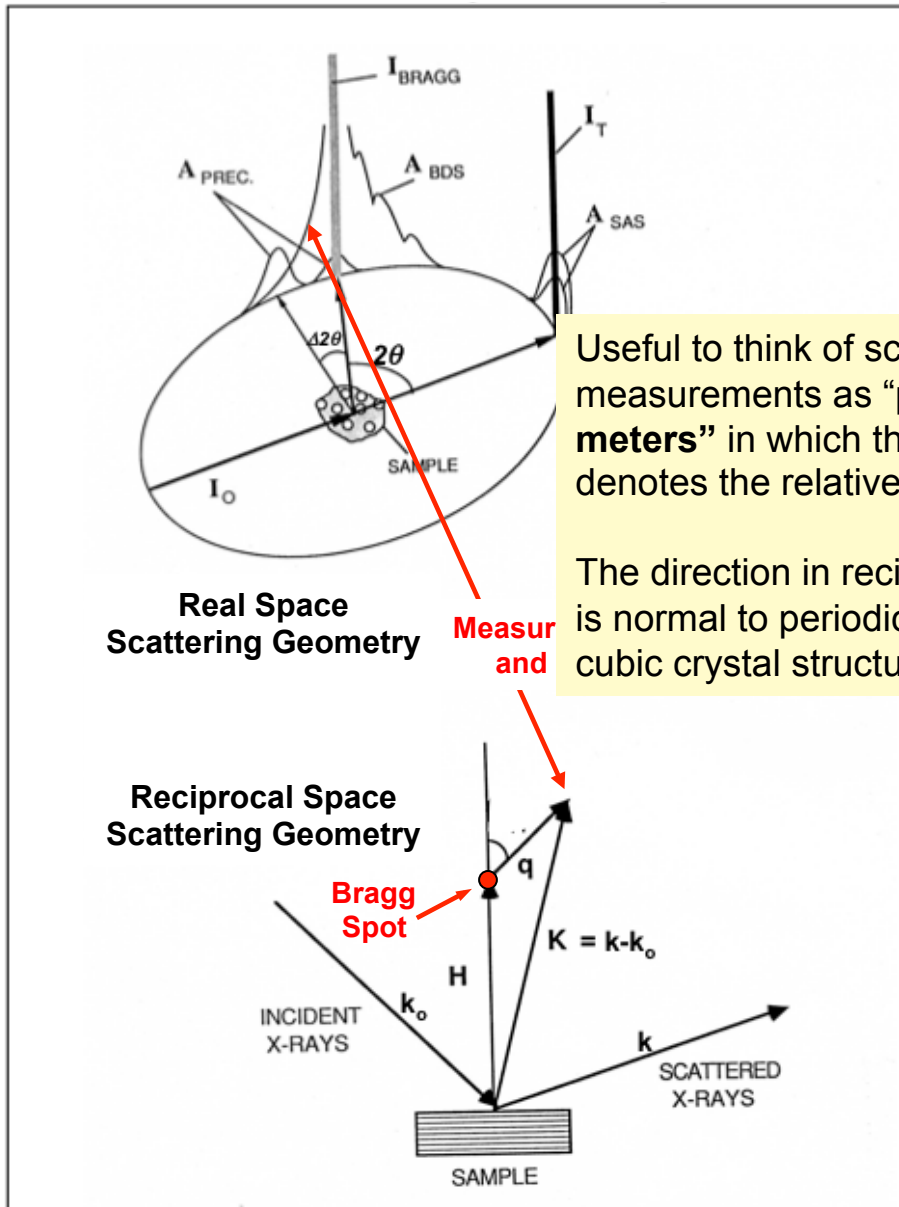
Defect Diffuse Scattering in Crystals

- Perfect crystals scatter x-rays into sharp peaks at Bragg reflections
- Distortions from lattice defects decrease Bragg peak intensities and distribute scattering between Bragg peaks according to the size and magnitude of the lattice disruption.



Real Space and Reciprocal Space (Fourier Transform) Connection

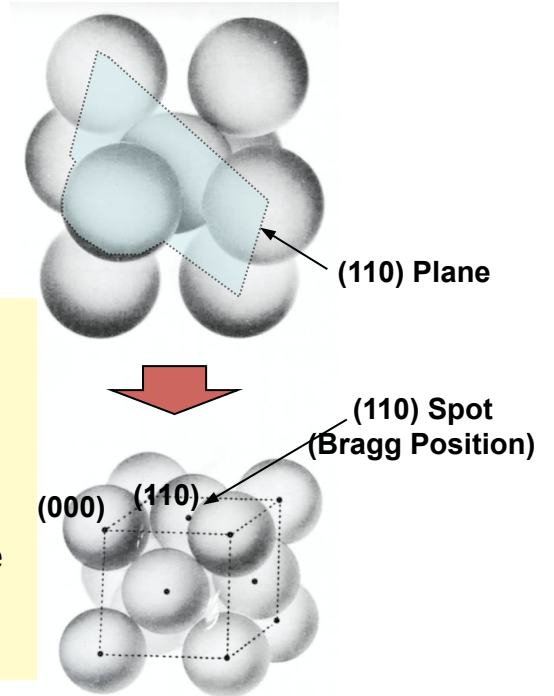
Real and Reciprocal Space Scattering Geometry



Useful to think of scattering measurements as “**periodicity meters**” in which the intensity denotes the relative volumes

The direction in reciprocal space is normal to periodic planes for cubic crystal structures

BCC Real Lattice



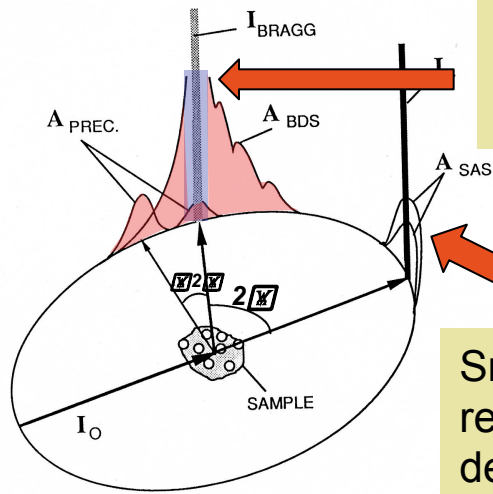
FCC Fourier Transform (FT) Lattice (i.e. Reciprocal Lattice)

Sharp spot FT lattice if the real lattice is perfect

Fuzzy spot FT lattice if the real lattice has distortions (i.e. Diffuse Scattering)

Diffuse Scattering As A Tool To Study Defects

Diffuse Scattering Geometry Schematic

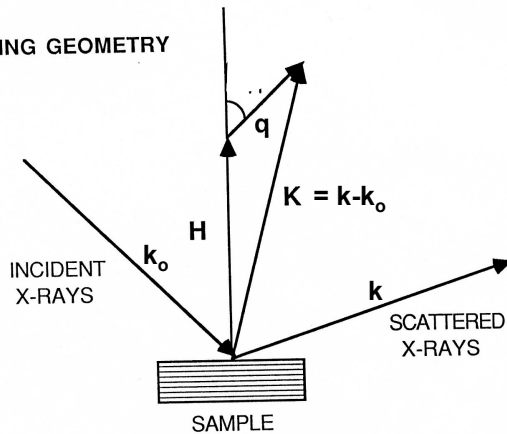


Bragg-diffuse scattering response to local rotation and strain fluctuations

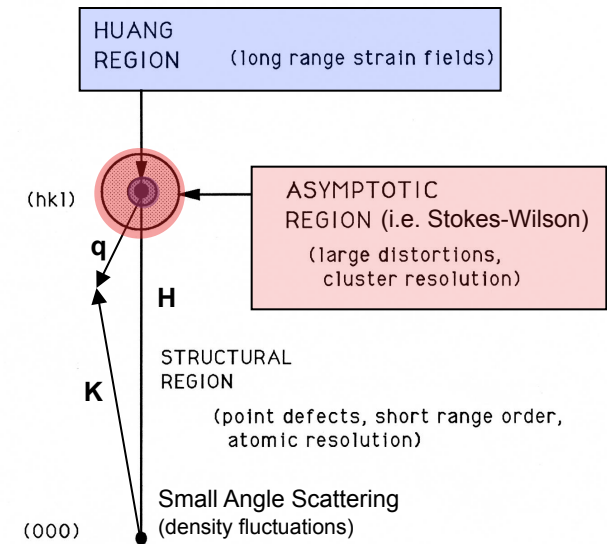
Small angle scattering response to electron density fluctuations

LARGE-ANGLE X-RAY SCATTERING FROM PRECIPITATES

SCATTERING GEOMETRY

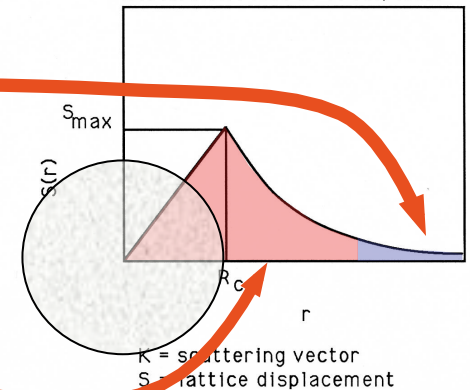


Diffuse Scattering Domain Schematic

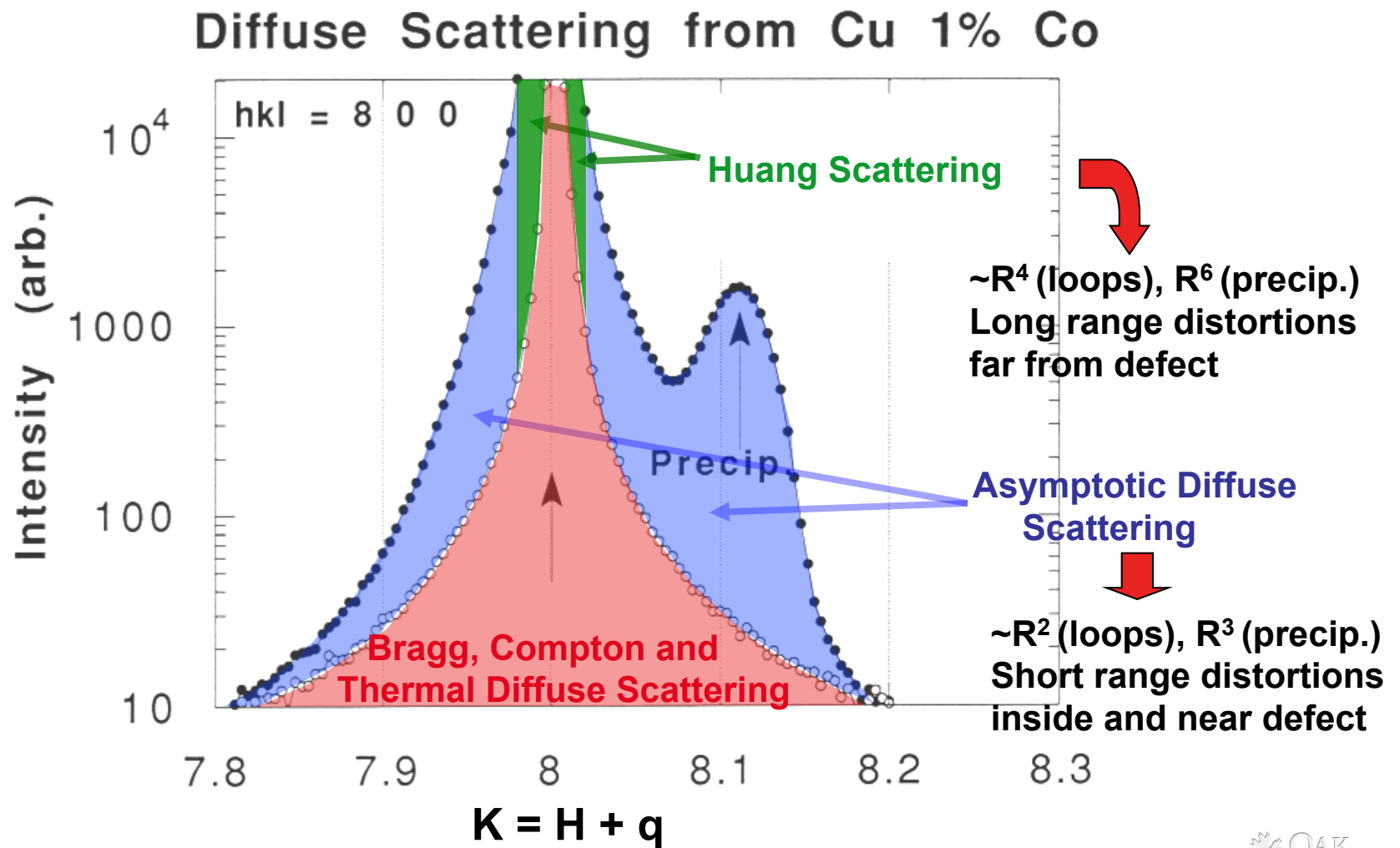


Real space origin of Huang scattering and asymptotic scattering

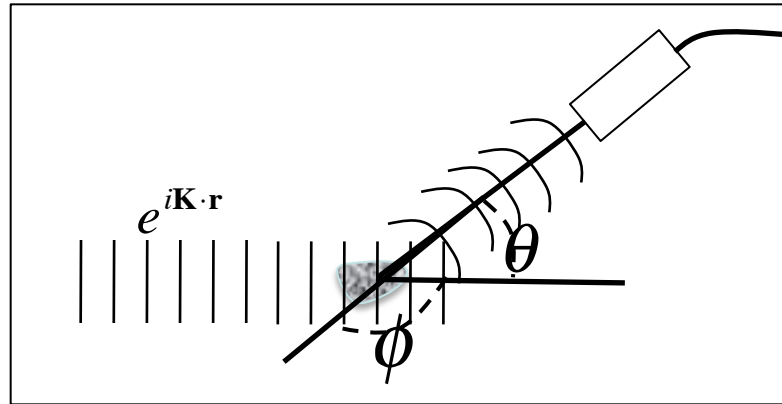
Distortion Field of Precipitate



Diffuse Scattering from Spherical Precipitates in Quenched and Aged Cu(1%)Co



Cross-Sections and Scattering Geometry



To quantify scattering, we consider an incoming plane wave with intensity I_0 particles/unit area/sec. We then measure (at angles θ, ϕ) the number of particles scattered into a solid angle $\Delta\Omega$, where $I(\theta, \phi)$ is the rate of particles detected and

$$\Delta\Omega = A_0 / R^2 = \frac{\text{Area of Detector}}{(\text{Distance from Sample})^2}$$

The scattering cross section for the sample is then defined by,

$$\frac{d\sigma(\theta, \phi)}{d\Omega} = \frac{I(\theta, \phi)}{I_0 \cdot \Delta\Omega}$$

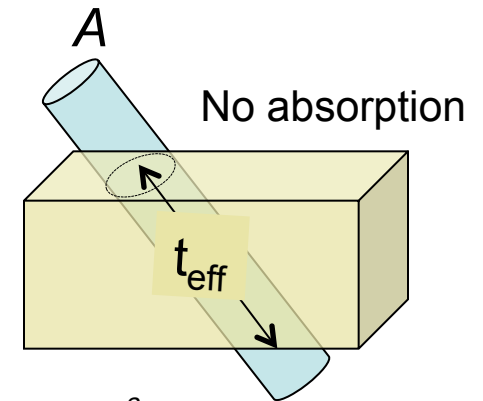
Therefore, it is necessary to know the solid angle $\Delta\Omega$ at the detector θ, ϕ and the incident beam intensity I_0 onto the sample.

Cross-Sections and Scattering Geometry (cont.)

- For N identical, randomly distributed defects or defect clusters

z

$$\begin{aligned} \frac{I(\theta, \phi)}{I_o} &= \frac{d\sigma(\theta, \phi)(\Delta\Omega)}{d\Omega} = \sum_{i=1}^N \frac{d\sigma_i(\theta, \phi)(\Delta\Omega)}{d\Omega} = N \frac{d\sigma_i(\theta, \phi)(\Delta\Omega)}{d\Omega} \\ &= N \frac{d\sigma_i(\theta, \phi)(\Delta\Omega)}{d\Omega} = \rho_D V_{sample} \frac{d\sigma_i(\theta, \phi)(\Delta\Omega)}{d\Omega} \end{aligned}$$



ρ_D = Density of defect scattering centers (defects/cm³)

v_{sample} = Effective sample volume (i.e. considering absorption)

$(\Delta\Omega)$ = Solid angle subtended by the detector (detector area/(distance²))

$I_o = \frac{P_o}{A}$ where P_o is the power and A is the cross-sectional area of the beam

$v_{sample} = A \cdot t_{eff}$, where t_{eff} is the effective thickness irradiated

(t_{eff} is the sample thickness along the incident beam for no absorption)

$$\frac{I(\theta, \phi)}{I_o} = \rho_D v_{sample} \frac{d\sigma_i(\theta, \phi)(\Delta\Omega)}{d\Omega} = \frac{I(\theta, \phi)}{\frac{P_o}{A}} = \rho_D A \cdot t_{eff} \frac{d\sigma_i(\theta, \phi)(\Delta\Omega)}{d\Omega}$$

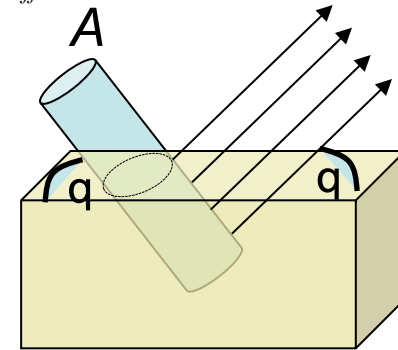
We then get (independent of A) the result : $I(\theta, \phi) = P_o \rho_D t_{eff} \frac{d\sigma_i(\theta, \phi)(\Delta\Omega)}{d\Omega}$

Cross-Sections and Scattering Geometry (cont.)

For the common cases of symmetric Bragg geometry and symmetric Laue geometry and samples with a finite linear absorption coefficient, μ (cm^{-1}), t_{eff} is given by

$$t_{\text{eff}} = \int_0^{\infty} e^{-2\mu_0 \frac{t}{\sin(\theta)}} \frac{dt}{\sin(\theta)} = \frac{1}{2\mu_0}$$

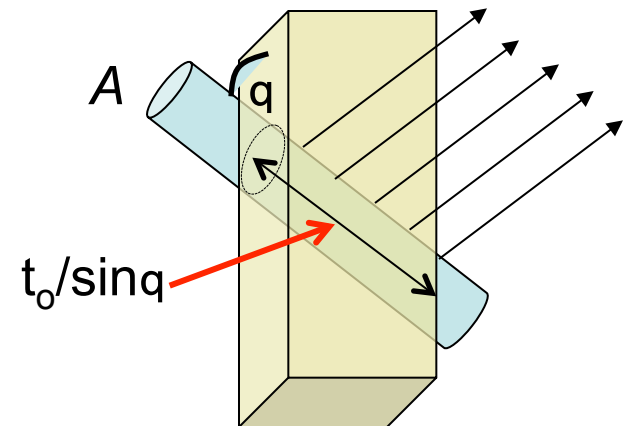
Symmetric Bragg Case



Bragg case with absorption

$$t_{\text{eff}} = \int_0^{t_0} e^{-\mu_0 \frac{t}{\sin(\theta)}} \frac{dt}{\sin(\theta)} = \frac{t_0}{\sin(\theta)} e^{-\mu_0 \frac{t_0}{\sin(\theta)}}$$

Symmetric Laue Case



Laue case with absorption

$$I(\theta, \phi) = P_o \rho_D \frac{d\sigma_i(\theta, \phi) (\Delta\Omega)}{d\Omega}$$

$\frac{1}{2\mu_0}$
Bragg

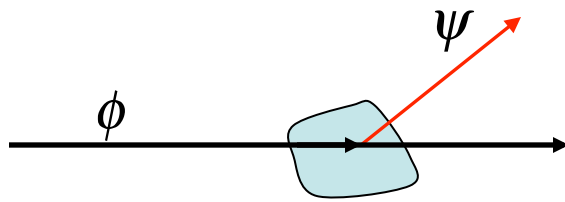
$\frac{t_0}{\sin(\theta)} e^{-\mu_0 \frac{t_0}{\sin(\theta)}}$
Laue

Separation of Bragg and Defect Diffuse Scattering

For the kinematic case the total scattering is given by:

$$\frac{d\sigma(\mathbf{K})}{d\Omega} = |r_e f(\mathbf{K})|^2 |A(\mathbf{K})|^2 = \left| \sum_i r_e f_i(\mathbf{K}) e^{i\mathbf{K}\cdot\mathbf{r}_i} \right|^2$$

X-rays $\sum_i r_e f_i e^{i\mathbf{K}\cdot\mathbf{r}_i}$
 Neutrons $\sum_i b_i e^{i\mathbf{K}\cdot\mathbf{r}_i}$



$$\psi^* \psi = |\psi|^2$$

Scattered Intensity
Perfect Crystal



$\langle |\psi|^2 \rangle$
Ensemble Average Intensity

$$\langle |\phi + \psi|^2 \rangle = \langle \phi^* \phi + \phi^* \psi + \psi^* \phi + \psi^* \psi \rangle$$



$$\langle |\phi + \psi|^2 \rangle = |\phi + \langle \psi \rangle|^2 + \langle |\psi|^2 \rangle - |\langle \psi \rangle|^2$$

Total **Bragg** **Diffuse**

A formal interference experiment shows (after adding and subtracting $\langle \psi^* \rangle \langle \psi \rangle = |\langle \psi \rangle|^2$ and rearranging) that only $\langle \psi \rangle$ is coherent and interferes with ϕ . [M. Lax, Rev. Mod. Phys. (1951); P. Dederichs, Solid State Physics (1972)]

$|\langle \psi \rangle|^2 \rightarrow$ Bragg Scattering

$\langle |\psi|^2 \rangle - |\langle \psi \rangle|^2 \rightarrow$ Fluctuation or Diffuse Scattering

$$\left[\frac{d\sigma(\mathbf{K})}{d\Omega} \right]_{Diffuse} = \left[\frac{d\sigma(\mathbf{K})}{d\Omega} \right]_{Total} - \left[\frac{d\sigma(\mathbf{K})}{d\Omega} \right]_{Bragg}$$

Single Defect Approximation for Diffuse Scattering

Associating ψ with the scattering amplitude $\sum_i r_e f_i e^{i\mathbf{K}\cdot\mathbf{r}_i}$, $\langle |\psi|^2 \rangle - |\langle \psi \rangle|^2$ leads to

$$\langle |\psi|^2 \rangle = \left\langle \left| \sum_i r_e f_i e^{i\mathbf{K}\cdot\mathbf{r}_i} \right|^2 \right\rangle = \left\langle \sum_{i,j} r_e^2 f_i f_j e^{i\mathbf{K}\cdot(\mathbf{r}_i - \mathbf{r}_j)} \right\rangle$$

$$|\langle \psi \rangle|^2 = \left| \left\langle \sum_i r_e f_i e^{i\mathbf{K}\cdot\mathbf{r}_i} \right\rangle \right|^2 = \left\langle \sum_i r_e f_i e^{i\mathbf{K}\cdot\mathbf{r}_i} \right\rangle \left\langle \sum_j r_e f_j e^{-i\mathbf{K}\cdot\mathbf{r}_j} \right\rangle$$

$$\left[\frac{d\sigma(\mathbf{K})}{d\Omega} \right]_{\text{Diffuse}} = \langle |\psi|^2 \rangle - |\langle \psi \rangle|^2 = \sum_{i,j} r_e^2 f_i f_j e^{i\mathbf{q}\cdot(\mathbf{r}_i^o - \mathbf{r}_j^o)} \left[\langle e^{i\mathbf{K}\cdot(\mathbf{s}_i - \mathbf{s}_j)} \rangle - \langle e^{i\mathbf{K}\cdot\mathbf{s}_i} \rangle \langle e^{-i\mathbf{K}\cdot\mathbf{s}_j} \rangle \right]$$

For defects on statistically random sites in the average (i.e. periodic) expanded lattice with a defect-induced static Debye-Waller factor, $L(\mathbf{K}) = c \sum [1 - \cos(\mathbf{K}\cdot\mathbf{s}(\mathbf{r}_i))]$,* diffuse scattering in the so-called “Single Defect Approximation” results:



$$\left[\frac{d\sigma(\mathbf{K})}{d\Omega} \right]_{\text{Diffuse}} = \left| \sum_j^{n^d} r_e f_j^d e^{i\mathbf{H}\cdot\mathbf{r}_j^d} e^{i\mathbf{q}\cdot\mathbf{r}_j^d} + \sum_i r_e f_i e^{-L(\mathbf{K})} e^{i\mathbf{q}\cdot\mathbf{r}_i} \left[e^{i\mathbf{K}\cdot\mathbf{s}(\mathbf{r}_i)} - 1 \right] \right|^2$$

Sum over atoms
in defect cluster

Sum over atoms in distorted
lattice surrounding cluster

Diffuse Scattering Cross-Section for Defect Clusters

$$\left[\frac{d\sigma(\mathbf{K})}{d\Omega} \right]_{Diffuse} = \left| \sum_j r_e f_j^d e^{i\mathbf{H}\cdot\mathbf{r}_j^d} e^{i\mathbf{q}\cdot\mathbf{r}_j^d} + \sum_i r_e f_i e^{-L(\mathbf{K})} e^{i\mathbf{q}\cdot\mathbf{r}_i} \left[e^{i\mathbf{K}\cdot\mathbf{s}(\mathbf{r}_i)} - 1 \right] \right|^2$$

$$\sum_i e^{i\mathbf{q}\cdot\mathbf{r}_i} \left[e^{i\mathbf{K}\cdot\mathbf{s}(\mathbf{r}_i)} - 1 \right] \equiv i\mathbf{K}\cdot\mathbf{s}(\mathbf{q}) + \sum_i e^{i\mathbf{q}\cdot\mathbf{r}_i} \left[\cos(\mathbf{K}\cdot\mathbf{s}(\mathbf{r}_i)) - 1 + i \sin(\mathbf{K}\cdot\mathbf{s}(\mathbf{r}_i)) - i\mathbf{K}\cdot\mathbf{s}(\mathbf{r}_i) \right]$$

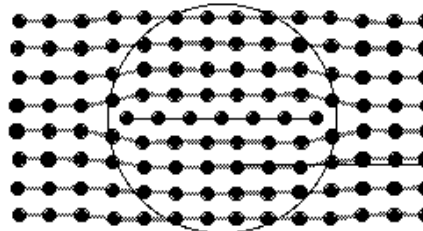
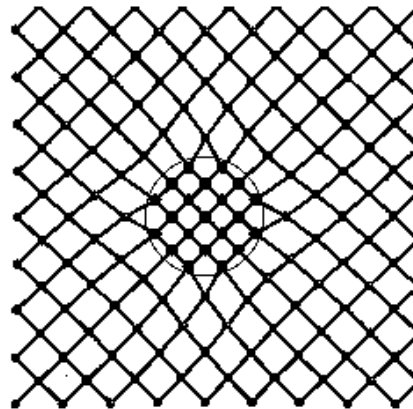
$$= i\mathbf{K}\cdot\mathbf{s}(\mathbf{q}) + \sum_i e^{i\mathbf{q}\cdot\mathbf{r}_i} \left[-(\mathbf{K}\cdot\mathbf{s}(\mathbf{r}_i))^2 / 2 + \text{higher order terms} \right]$$

$\mathbf{K}\cdot\mathbf{s}(\mathbf{q})$ is known analytically and $\mathbf{s}(\mathbf{r}) \sim 1/r^2$ for finite clusters, so the lattice sum converges rapidly

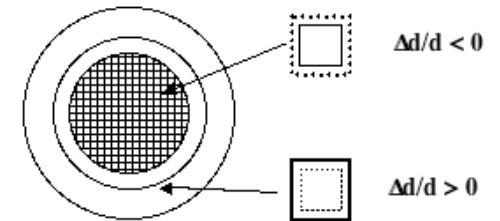


Accurate scattering cross-sections require the use of numerically calculated displacement fields $\mathbf{s}(\mathbf{r})$

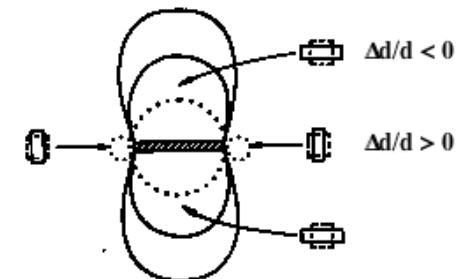
This is very important to get accurate sizes & densities



Coherent Precipitate

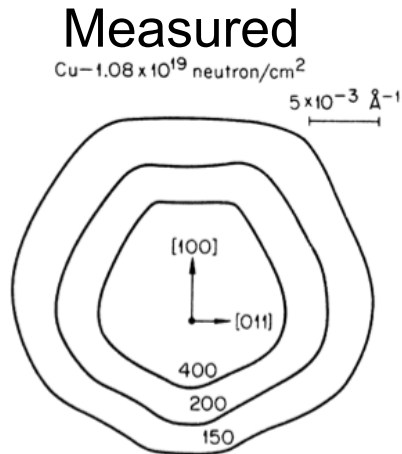


Dislocation Loop



Diffuse Scattering from Spherical Precipitates in Aged Cu(1%)Co

Loops in irradiated copper



Spherical precipitates in aged Cu(1%)Co

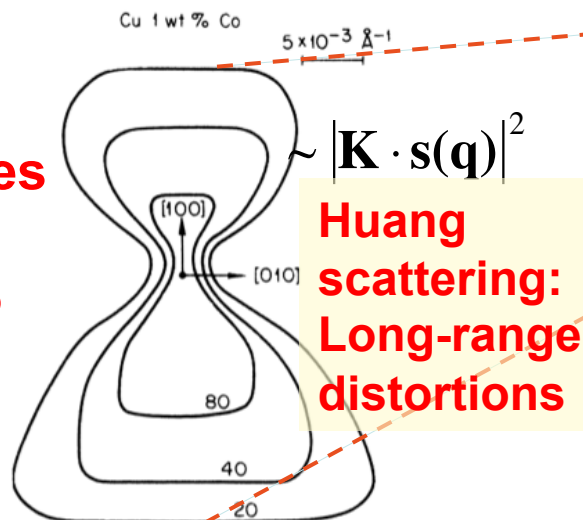


FIG. 2. Measured diffuse scattering contours near the (200) reflection from neutron-irradiated copper and Cu:1-wt%-Co.

Precipitate Direct Scattering

Calculated

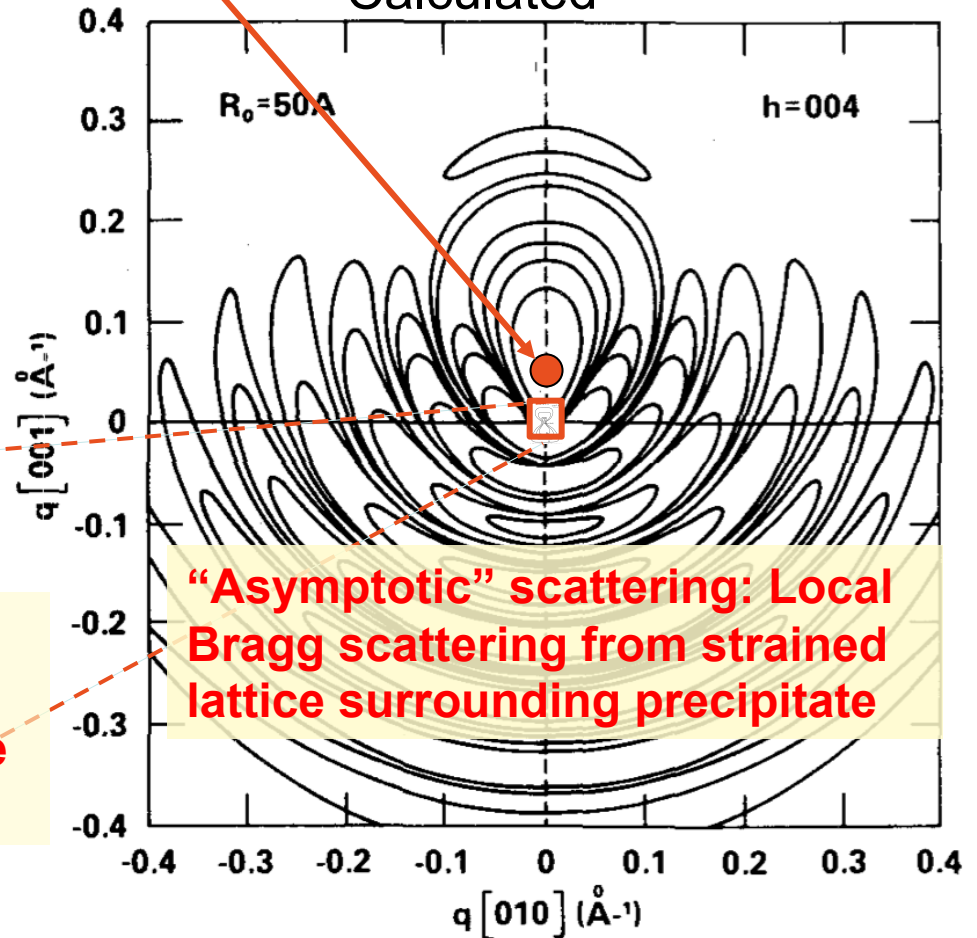
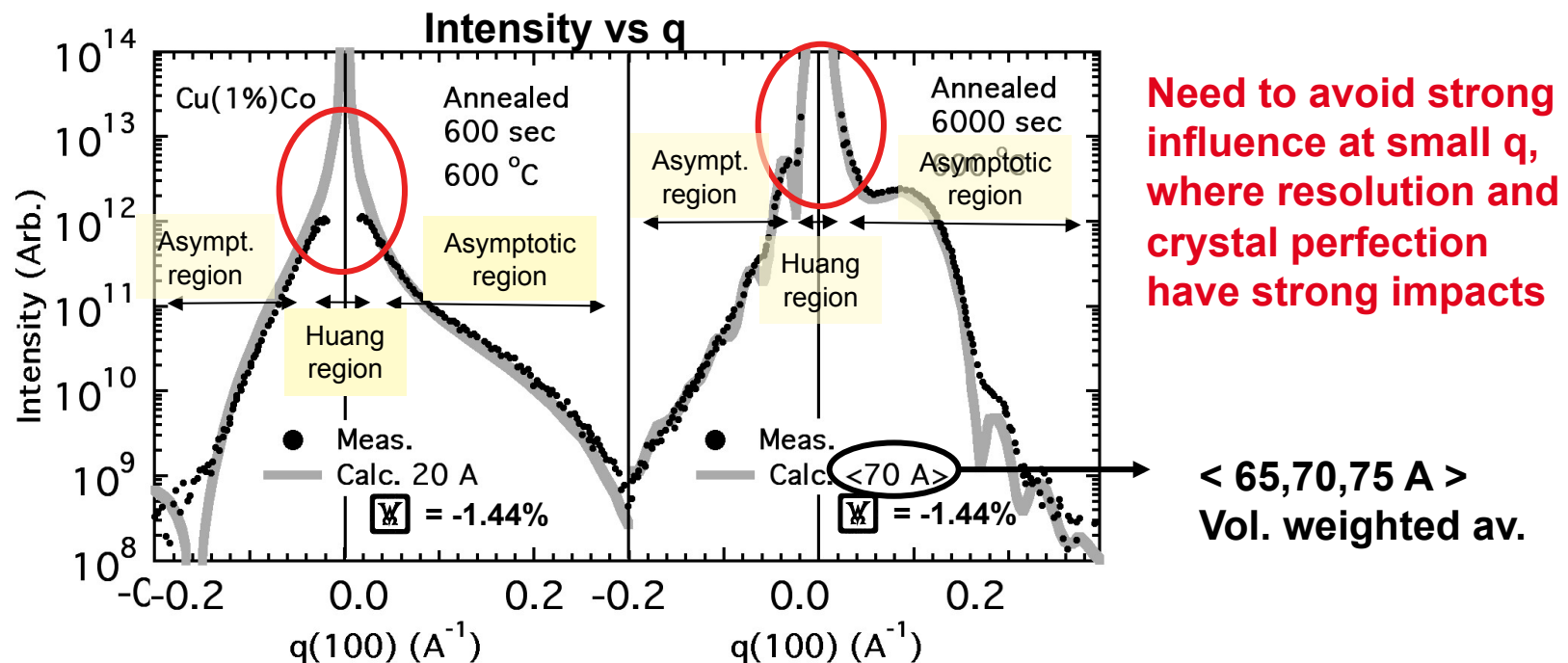


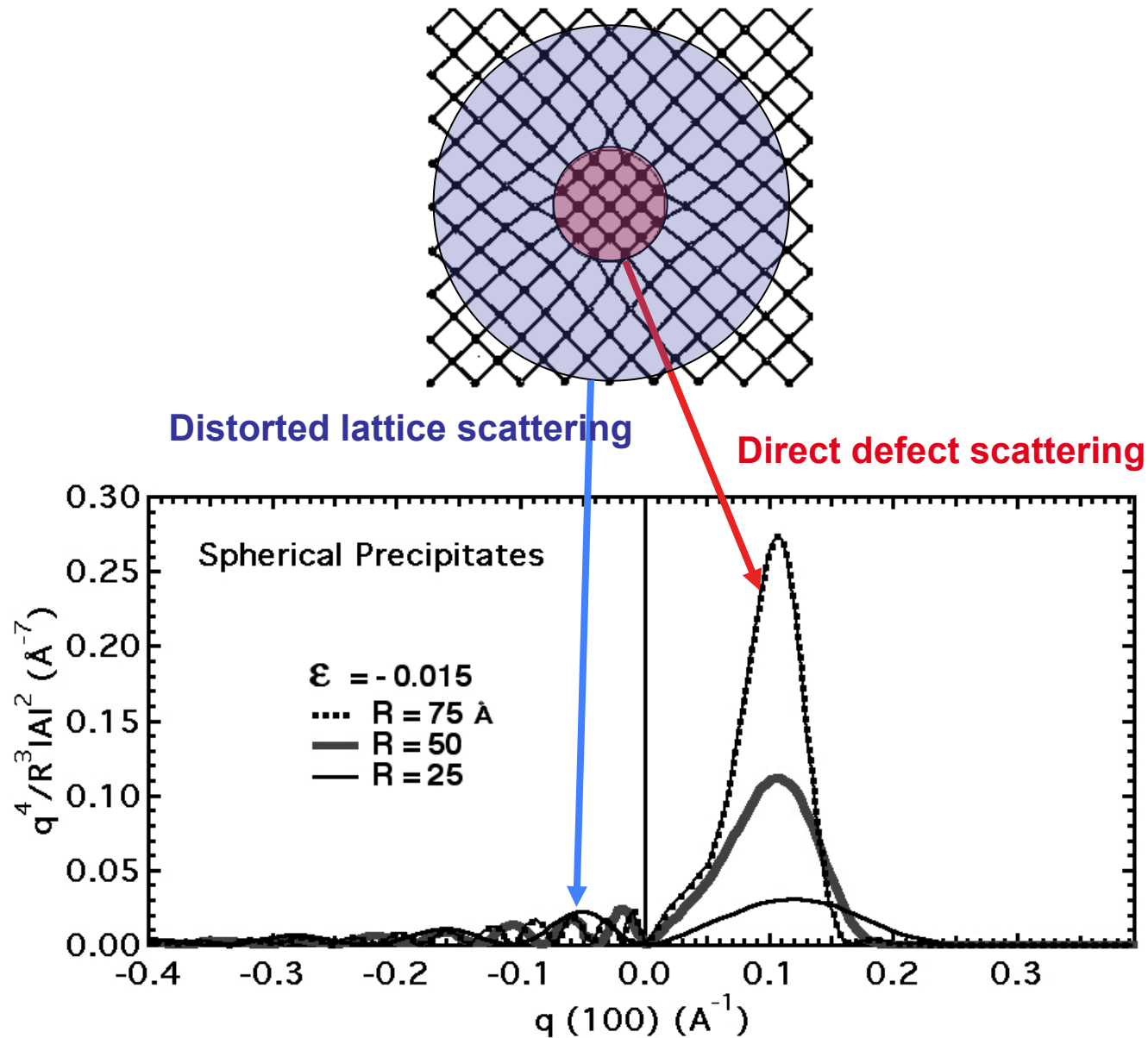
FIG. 4. Qualitative isointensity plot of the scattering cross section near the (004) reflection for a 50 Å precipitate with $\epsilon = -0.015$.

Diffuse Scattering for Cobalt Precipitates in Copper

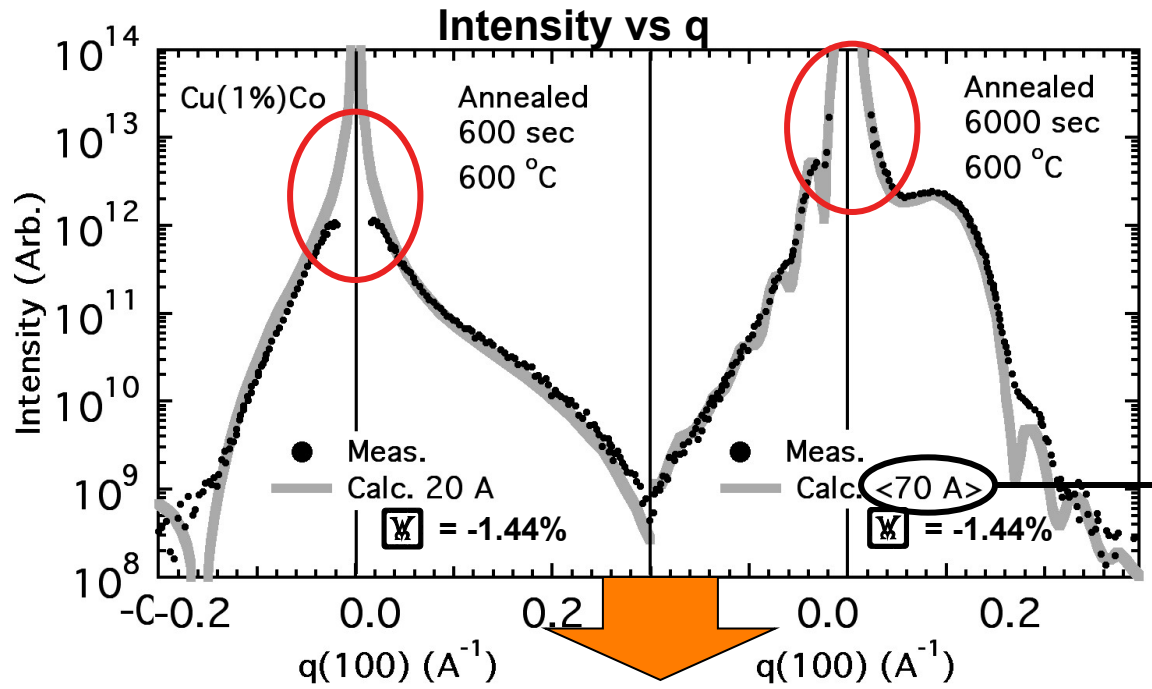


- The small- q (Huang) region measures a high moment of defect radius and no direct size information
- The measurement resolution (i.e. detector solid angle subtended) may not be small enough obtain reliable information at small q .
- The so-called “asymptotic” region where the “local-Bragg” scattering interpretation is valid provides the most direct, most reliable, and most detailed information on defect cluster size distributions.
- q^4 weighting minimizes the less informative intensities at small q .

q^4 Weighted Calculated Diffuse Scattering Cross-Section for Spherical Precipitates in An Isotropic Medium

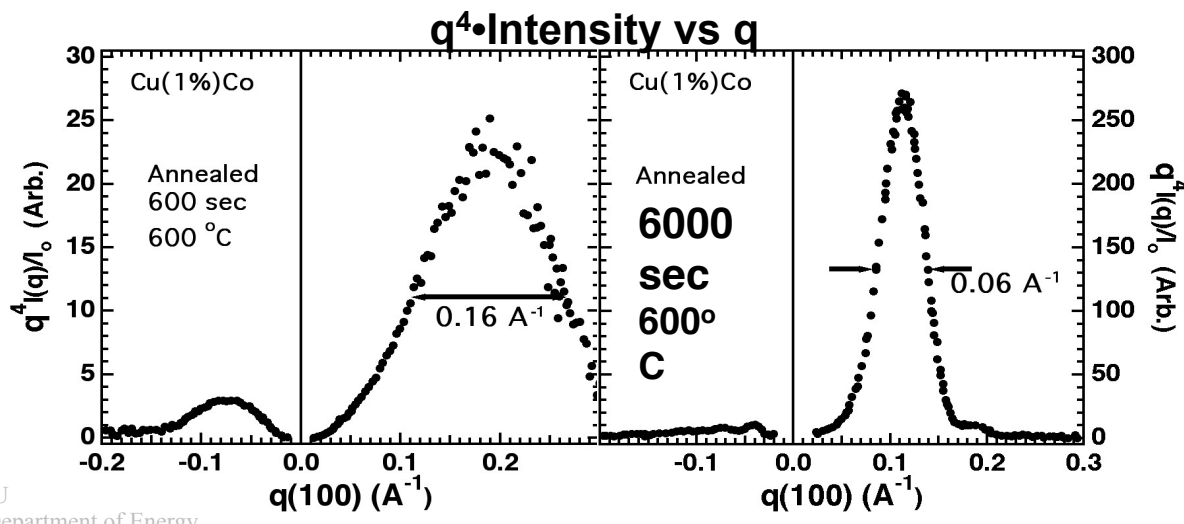


Diffuse Scattering for Cobalt Precipitates in Copper



Need to limit strong influence at small q , where resolution and crystal perfection have strong impacts

$\langle 65, 70, 75 \text{ \AA} \rangle$
Vol. weighted av.



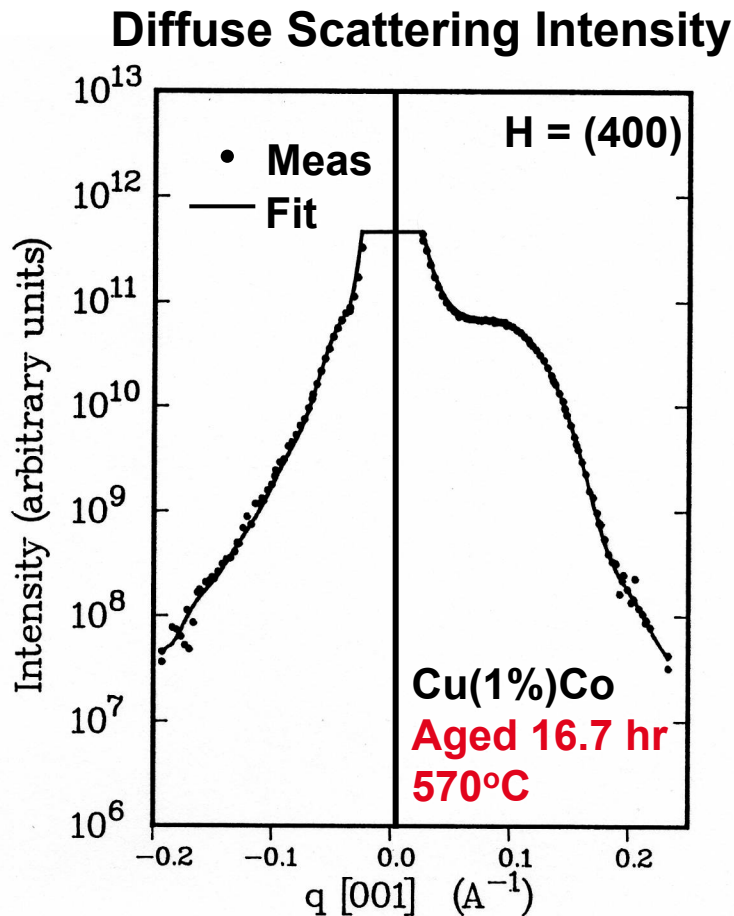
q^4 weighting puts intensities on a linear scale, it emphasizes the direct scattering from the defect, and resolution is less critical

Determination of The Size Distribution for Coherent Cobalt Precipitates in Aged Cu(1%)Co

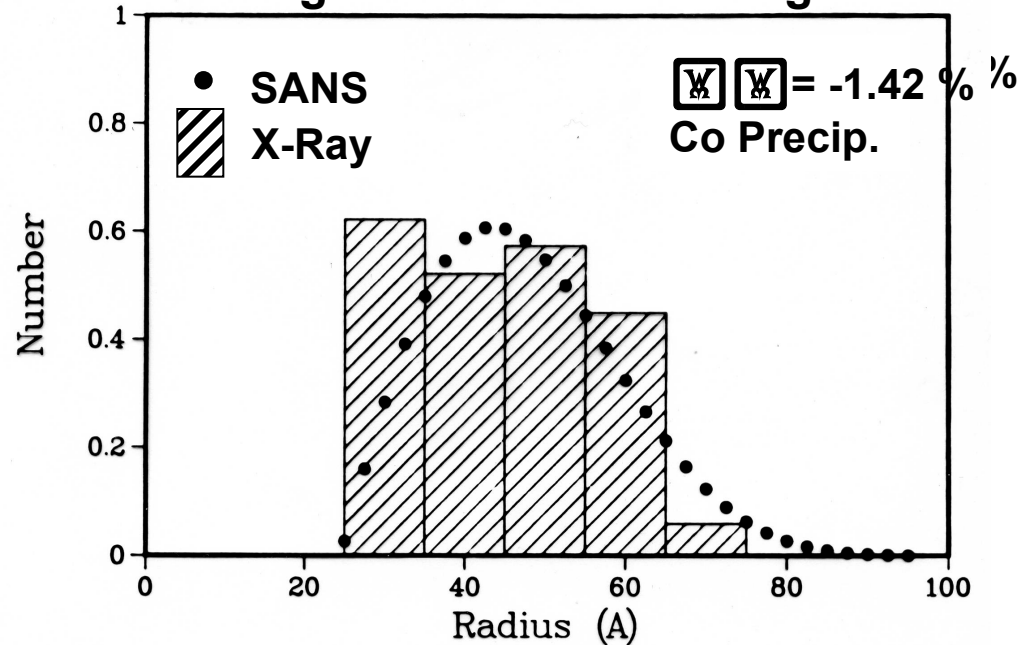
$$I(\mathbf{K}) = \frac{I_o}{2\mu_o} \sum_i c_i(R_i) \frac{d\sigma_i(\mathbf{K}, R_i)}{d\Omega} (\Delta\Omega)$$



Fit $c_i(R_i)$ to measured intensity using numerically calculated cross-sections $\frac{d\sigma_i(\mathbf{K}, R_i)}{d\Omega}$

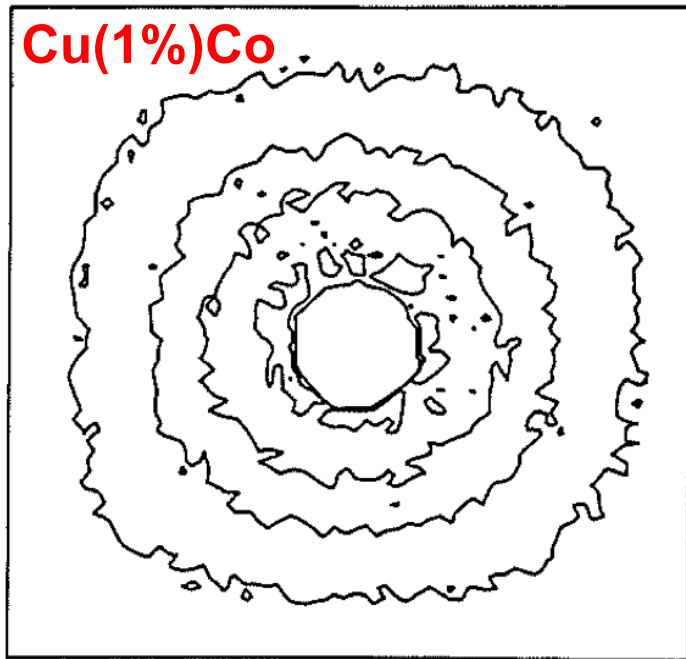


Precipitate Size Distribution Compared to Small Angle Neutron Scattering Results

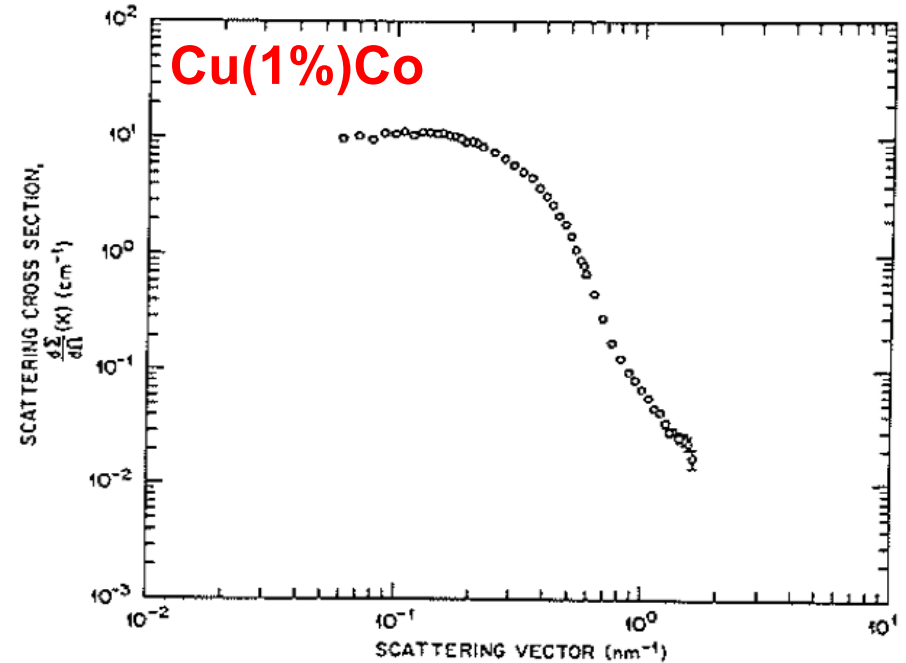


Spoooner, Iida, & Larson, in *Characterization of Defects in Materials*, MRS 82, 79 (1987); MRS 82, 73 (1987)

Small Angle Neutron Scattering (SANS) Study of Coherent Cobalt Precipitates in Aged Cu(1%)Co



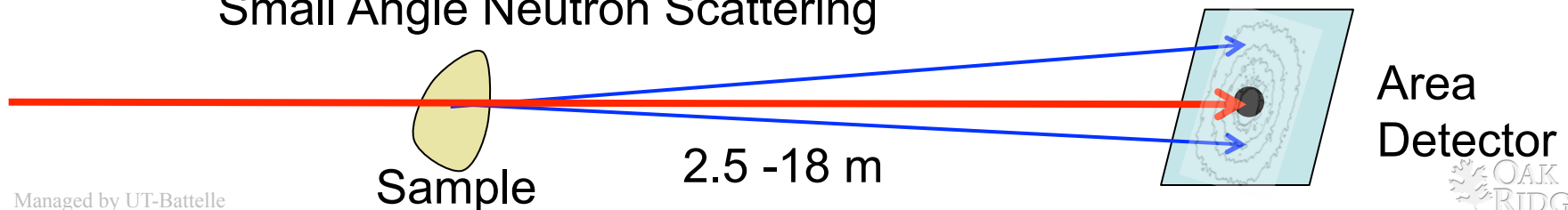
SANS intensity contours on area detector at 6 m



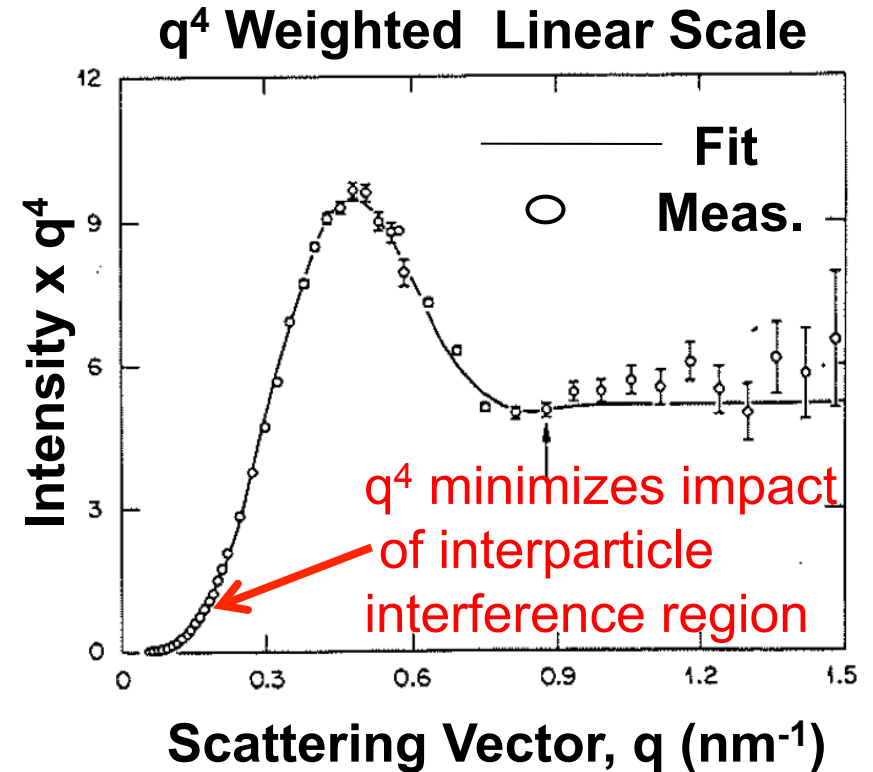
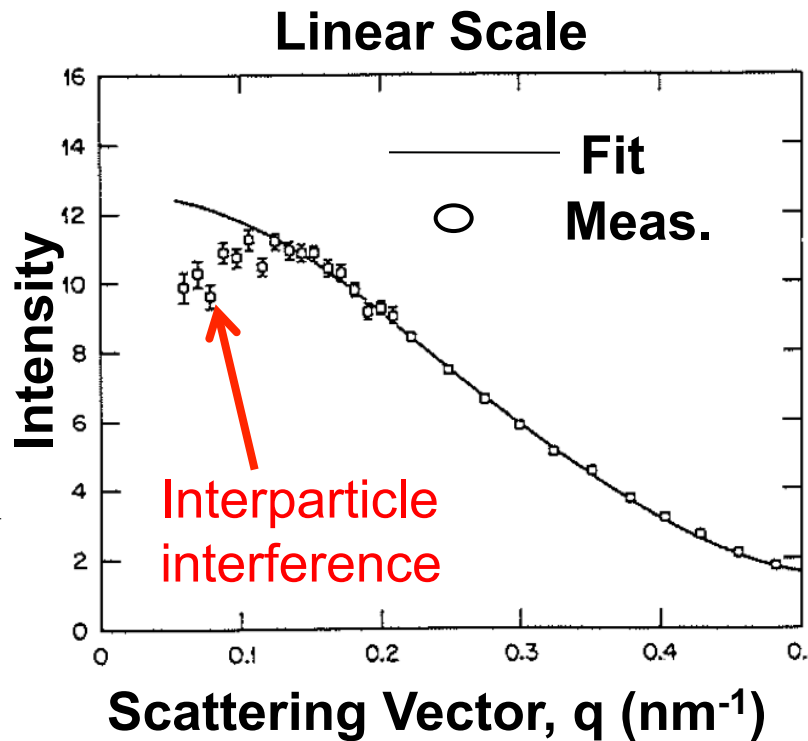
Radially-averaged SANS intensities for 2.5, 6, and 18 m measurements

- Small angle scattering represents (000) reflection – Scattering density

Small Angle Neutron Scattering

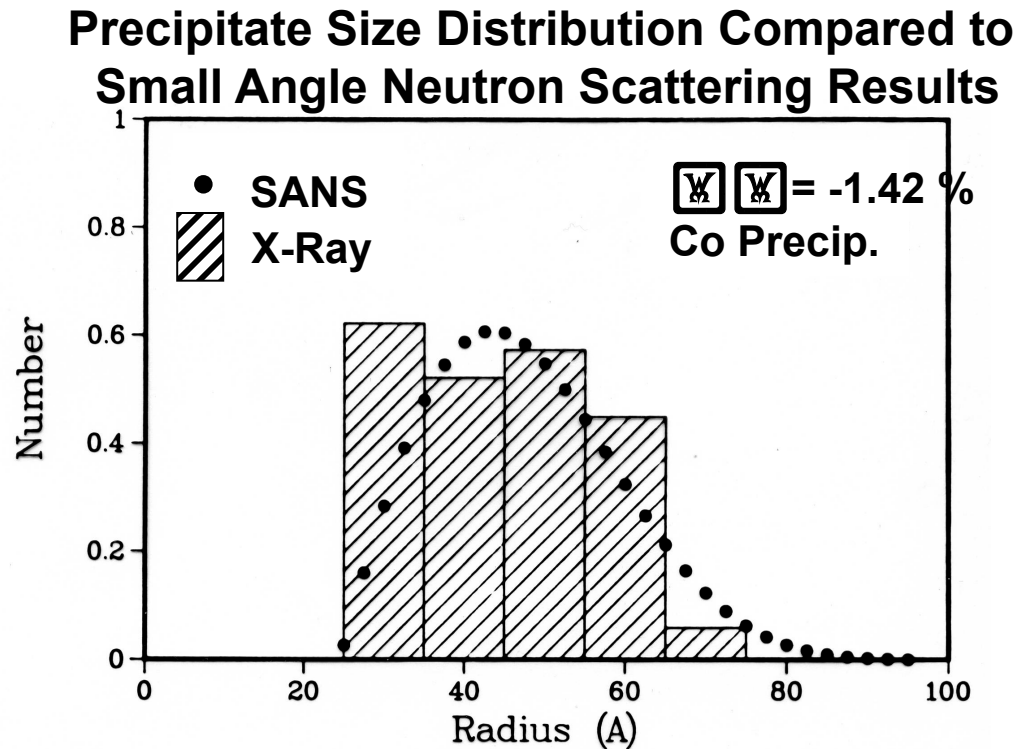


Small Angle Neutron Scattering (SANS) Cu(1%)Co: Linear and q^4 Weighted Scales; Measured and fitted



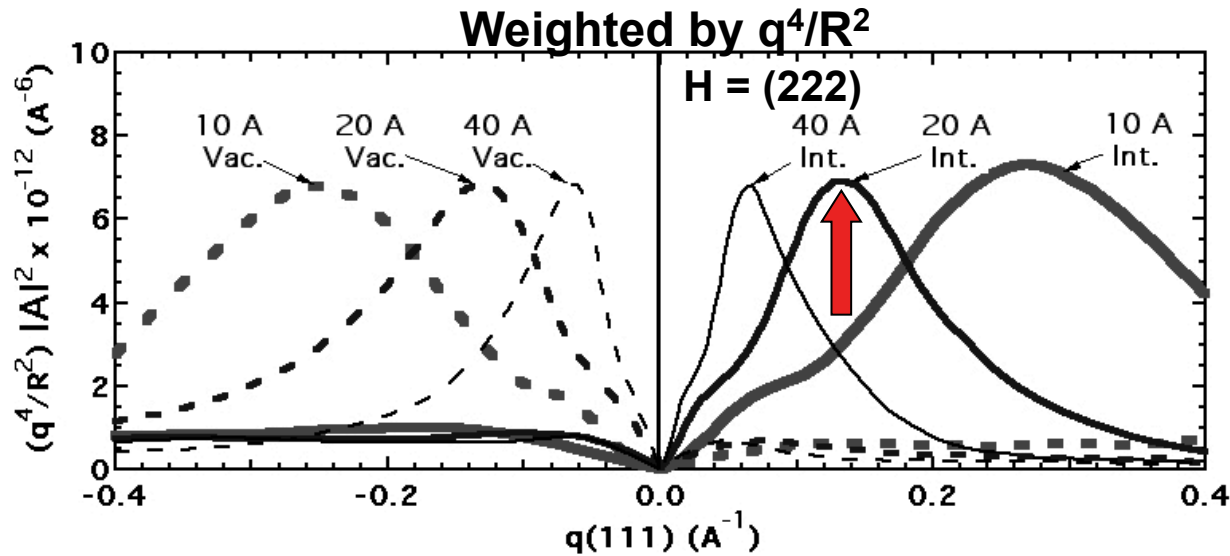
- Small angle scattering sensitive to scattering density fluctuations the relative to the host material, which is the precipitate particle in this case
- Interparticle interference is result of the fact that particles cannot be truly randomly positioned because they cannot overlap

Recalling Comparison of Small Angle Neutron Scattering (SANS) and X-Ray Bragg Diffuse Scattering Size Distributions

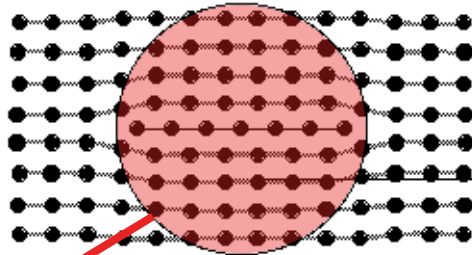


Spooner, Iida, & Larson, in *Characterization of Defects in Materials*, MRS 82, 79 (1987): MRS 82, 73 (1987)

Scattering Cross-Sections Calculated for Interstitial And Vacancy Loops in Copper



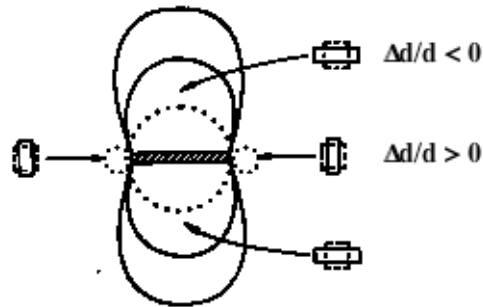
Note that q^4/R^2 removes the Huang divergence at $q=0$ and normalizes the scattering to the number of point defects in the loops



$$\epsilon \approx -\frac{b}{4R}$$



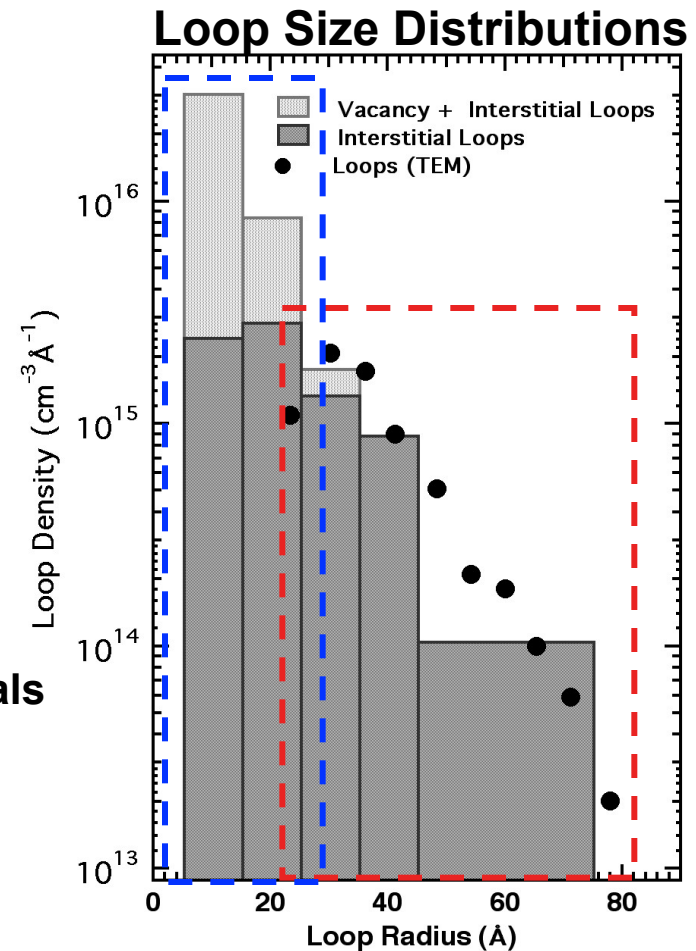
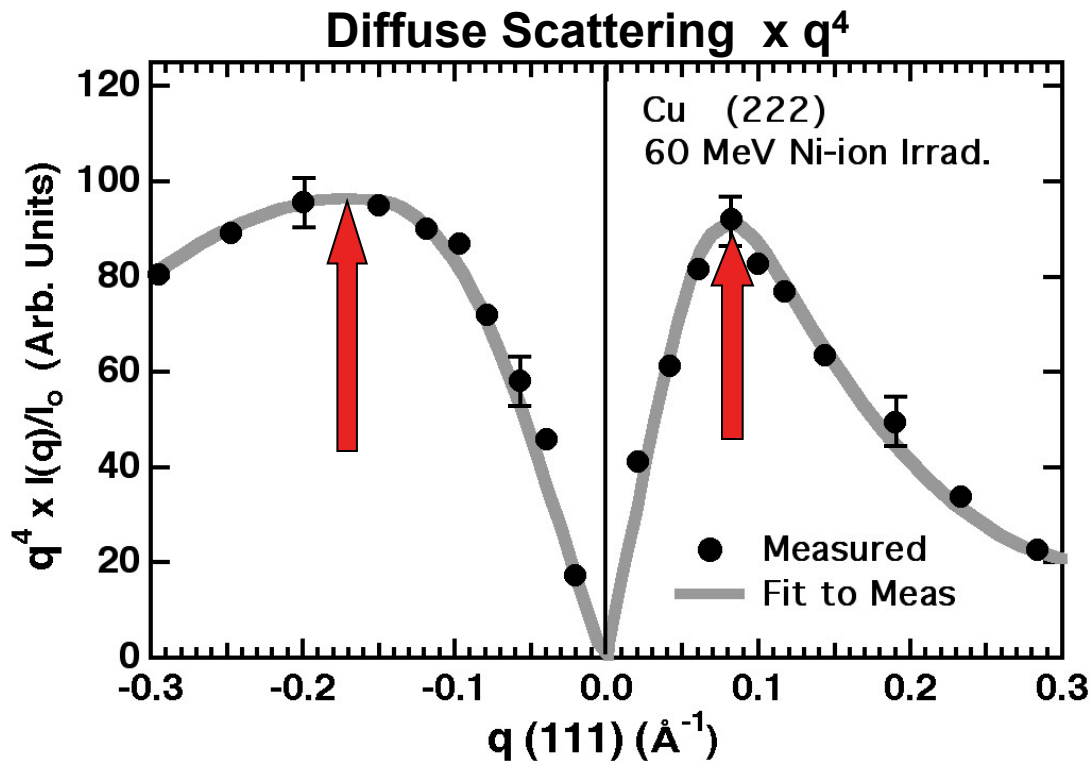
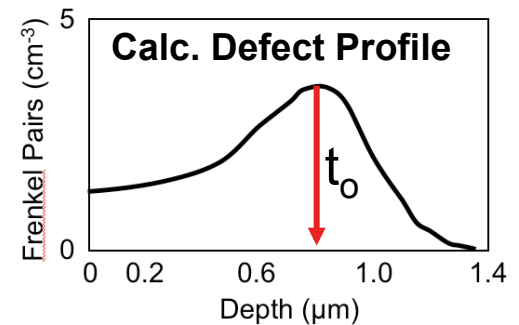
$$\epsilon = -\frac{b}{4R} \Rightarrow \frac{2.08}{80} = -0.026 \text{ for } R = 20\text{A}$$



$$\epsilon = -\frac{q}{K_{222}} \Rightarrow \frac{0.135}{6.04} = -0.029 \text{ for } R = 20\text{A}$$

Interstitial and Vacancy Loops in Ion Irradiated Ni

$$I(\mathbf{K}) = \frac{I_o}{\sin(\theta)} \sum_i c_i(t_o, R_i) \frac{d\sigma_i(\mathbf{K}, R_i)}{d\Omega} (\Delta\Omega) \int_0^\infty \frac{c_i(t)}{c_i(t_o)} e^{-2\mu_o t / \sin(\theta)} dt$$



- Equal intensities for positive and negative q implies substantially equal numbers of vacancies and interstitials
- Vacancy loop sizes are smaller than interstitial loops
- X-Ray and TEM size distributions agree for R > 20 Å
- TEM observations miss most vacancy loops/clusters

Interstitial and Vacancy Loops in 4 K Neutron Irradiated Cu and After 60-300 K Anneals

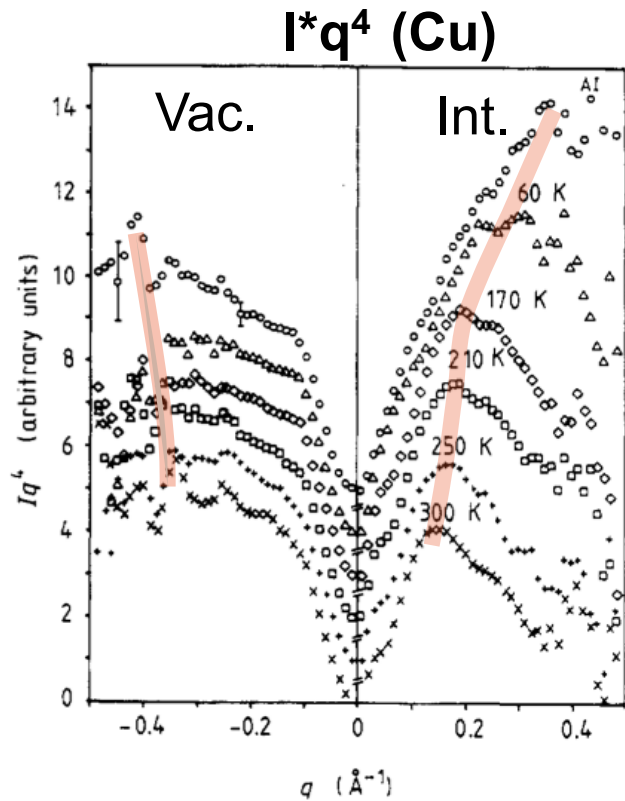


Figure 4. Defect-induced diffuse intensity scaled by q^4 in Cu, after irradiation (curve AI), and after recovery at the different temperatures T_A as indicated.

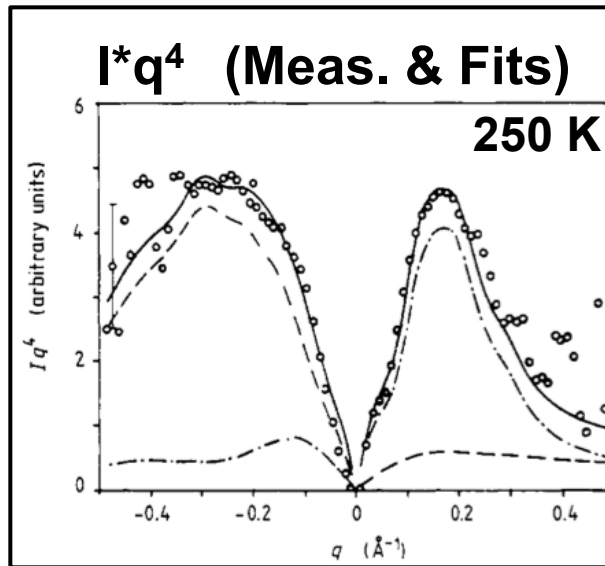


Figure 5. Defect-induced diffuse intensity scaled by q^4 in Cu after recovery at 250 K: \circ , experimental data; —, theoretical result of best fit; - - -, contribution from interstitial loops; - · - ·, contribution from vacancy loops.

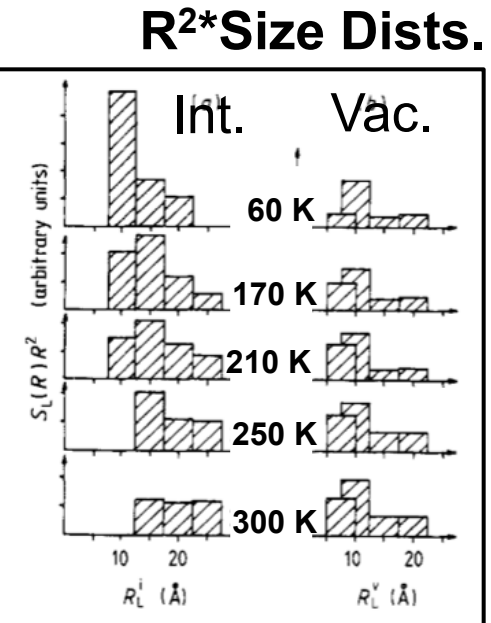
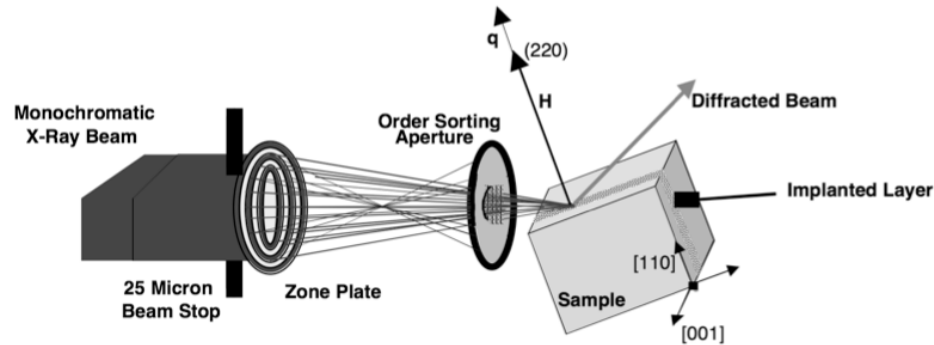


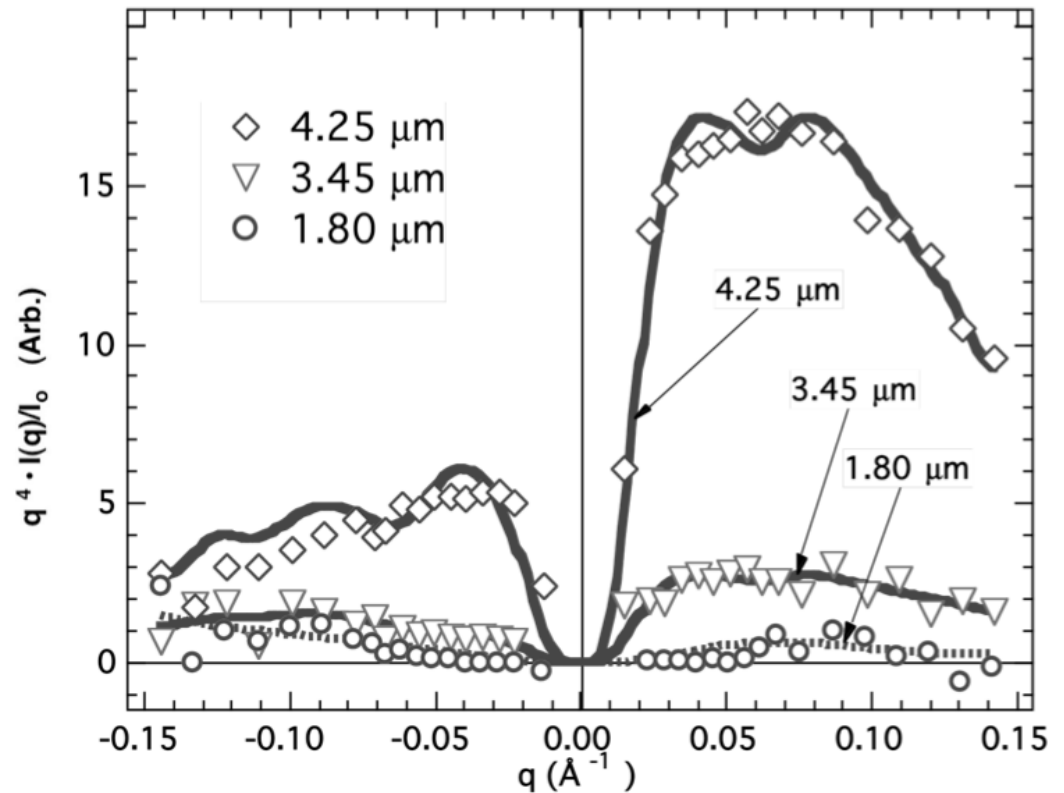
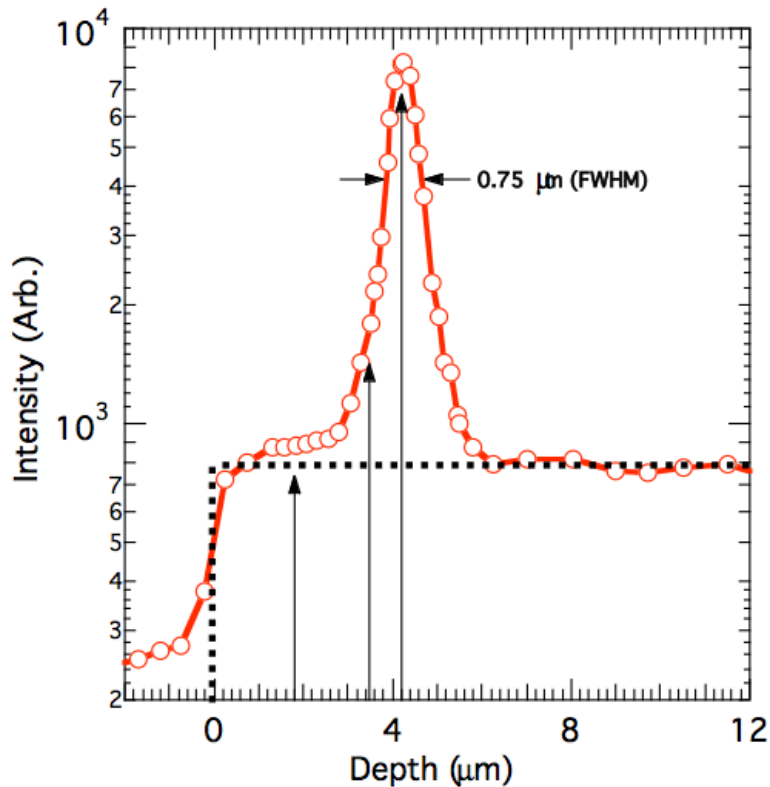
Figure 6. Loop size distribution $S_L(R)$ scaled by R^2 as obtained from the best fit to experimental data: (a) interstitial loops; (b) vacancy loops.

- q^4 weighted scattering (left) indicates vacancy and interstitial loops in 4K neutron irradiated Cu for 60 -300k anneals
- The maxima in the interstitial loop scattering (left) tends to smaller q (i.e. larger radii) with higher temperature
- The intensity maxima for vacancy loops (left) change only slightly with annealing temperature
- The size distributions for vacancy and interstitial loops (right) indicate interstitial agglomeration but no vacancy agglomeration

Submicron Depth Resolved Diffuse Scattering Measurements in 10 MeV Self-Ion Irradiated Si

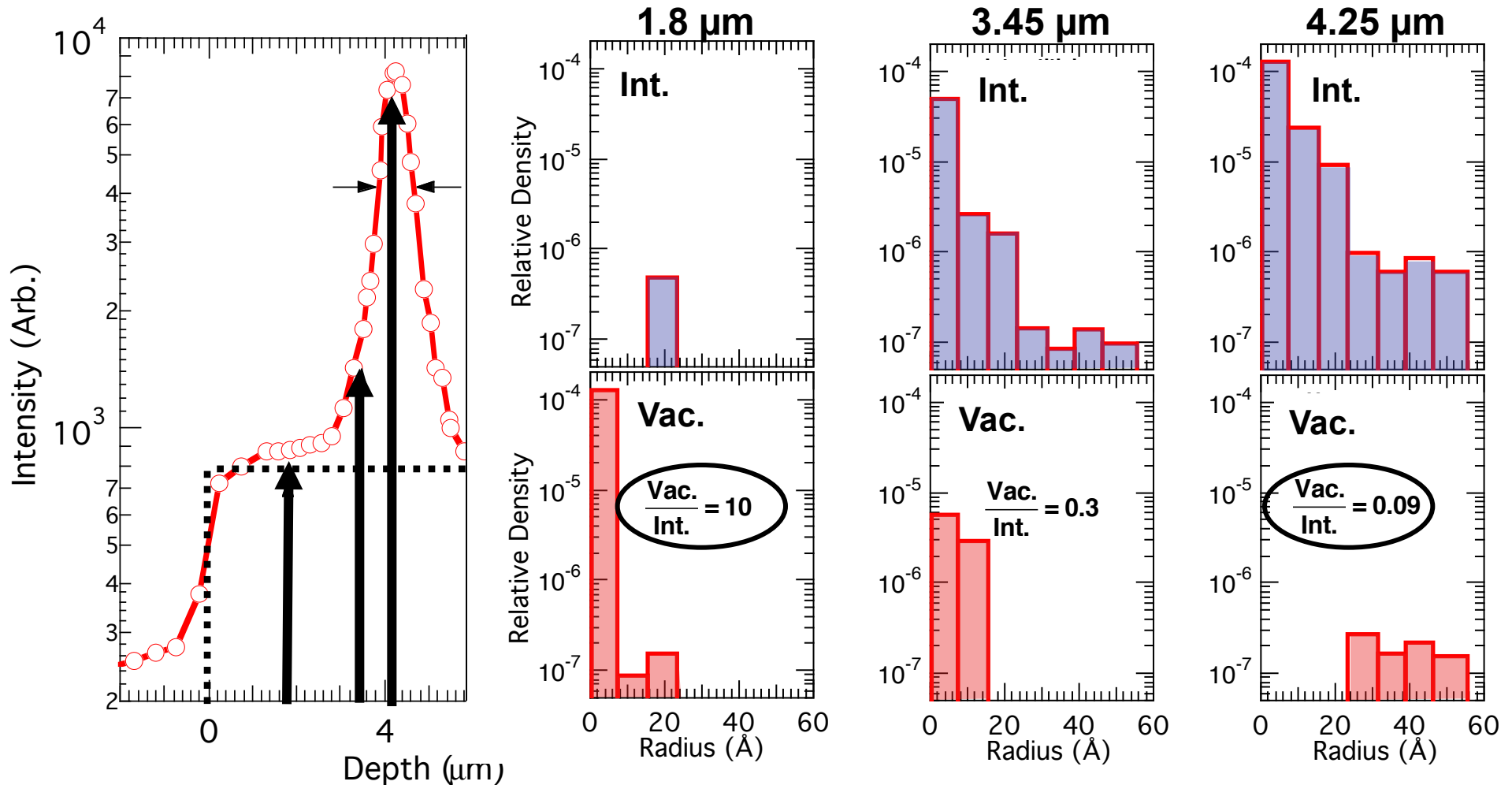


Diffuse Intensity Depth Profile



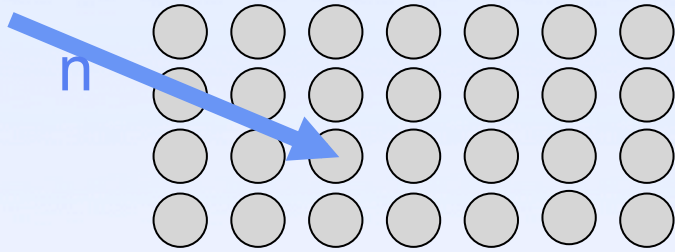
for [Updated analysis from: Yoon, Larson, et al, Appl. Phys. Lett. 75, 2791 (1999)]

Size Distributions and Ratio of Vac./Int. in Self-Ion Irradiated Si as A Function of Implantation Depth



- The fraction of vacancies is 10x larger near the surface
- The fraction of vacancies is 10x smaller near the Si-ion end of range
- This result is consistent with the so-called **vacancy implanter effect**

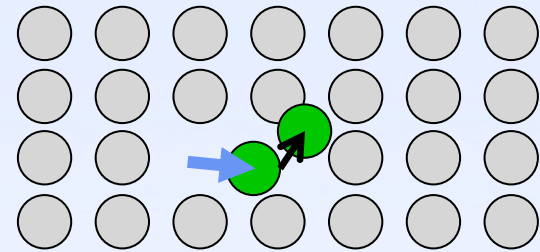
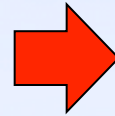
Atomic Displacement Cascade Dynamics



Direct collision of fast neutron with crystal atom

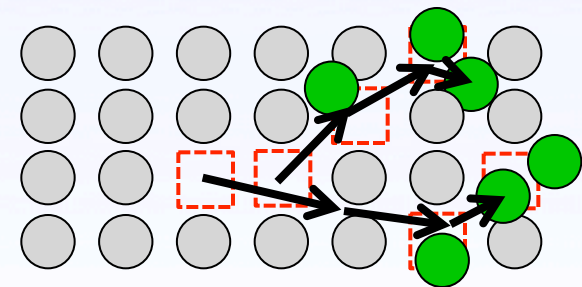
Fundamental origin of radiation damage occurs
On Picosecond Time Scale

But residual defects Evolve for Gigaseconds



300 million degree atom recoil

Femtosecond time-scale

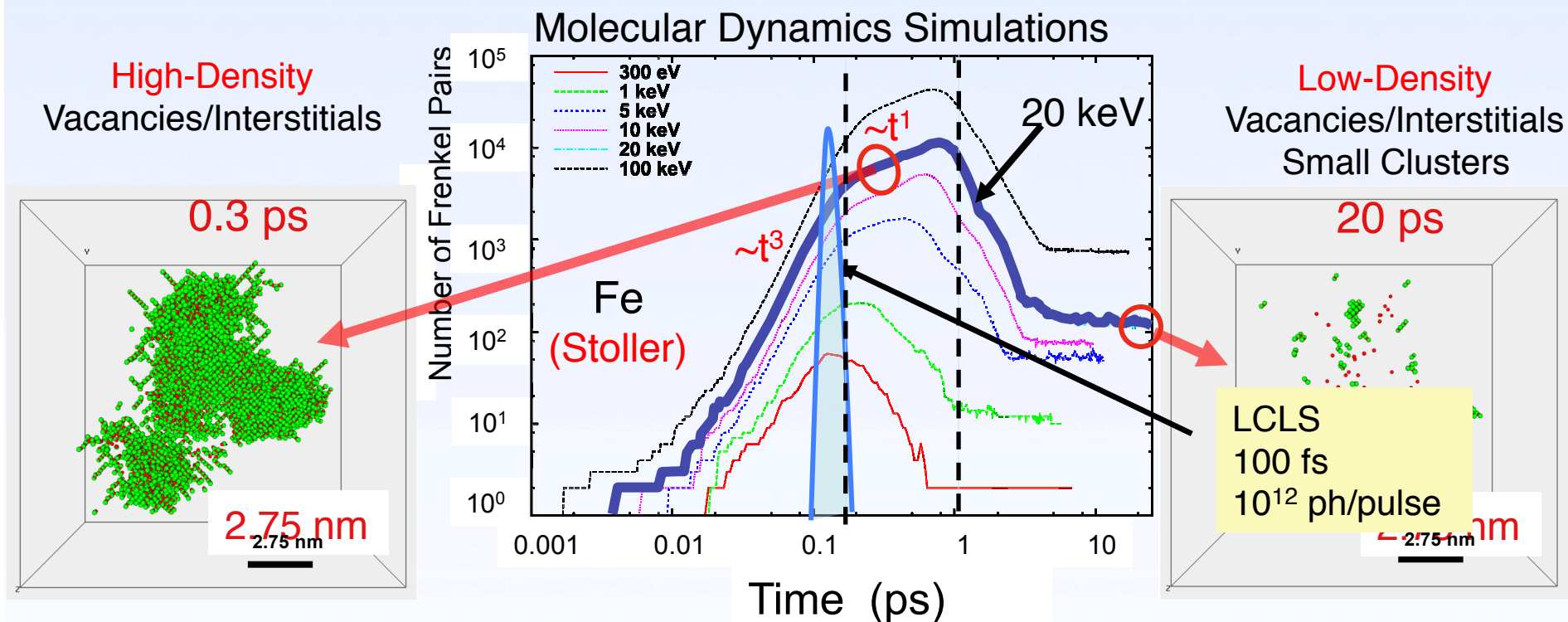


Cascade of atomic recoils

Picosecond time-scale

Very Large Number of Molecular Dynamics Simulations of Cascades - Over 50 Years

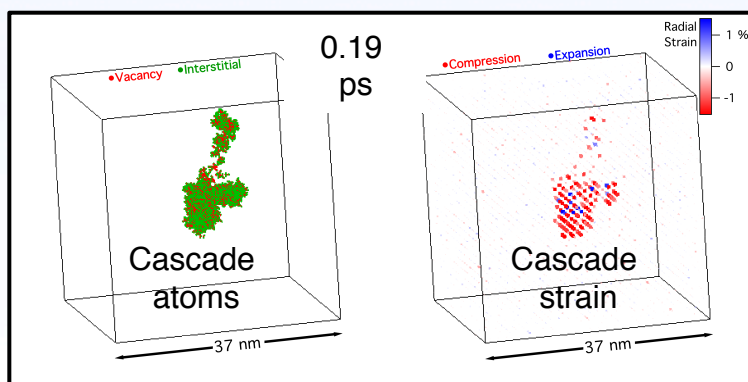
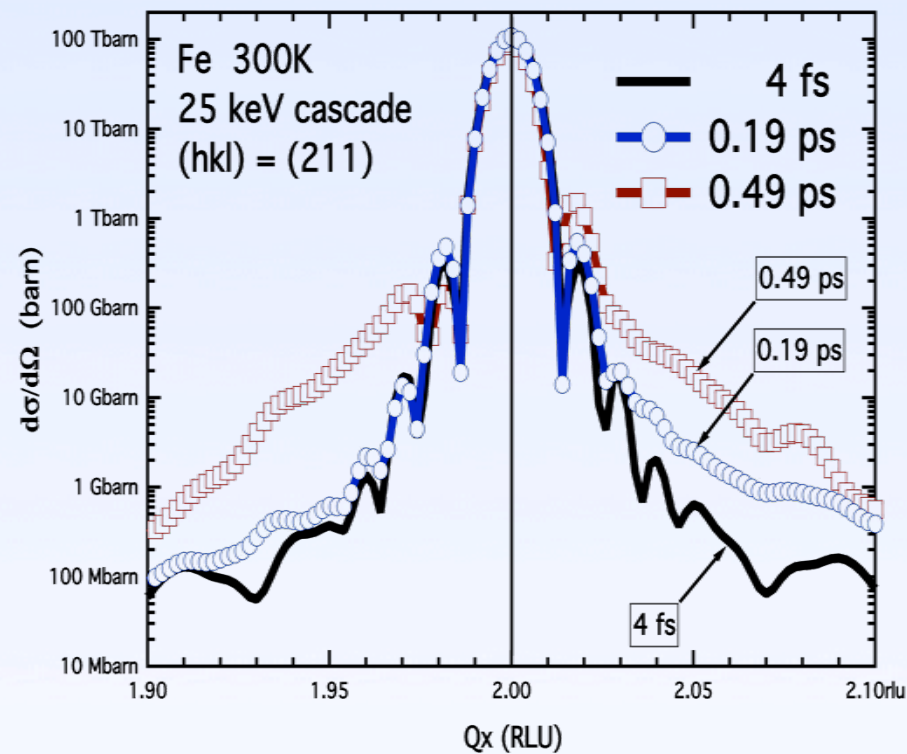
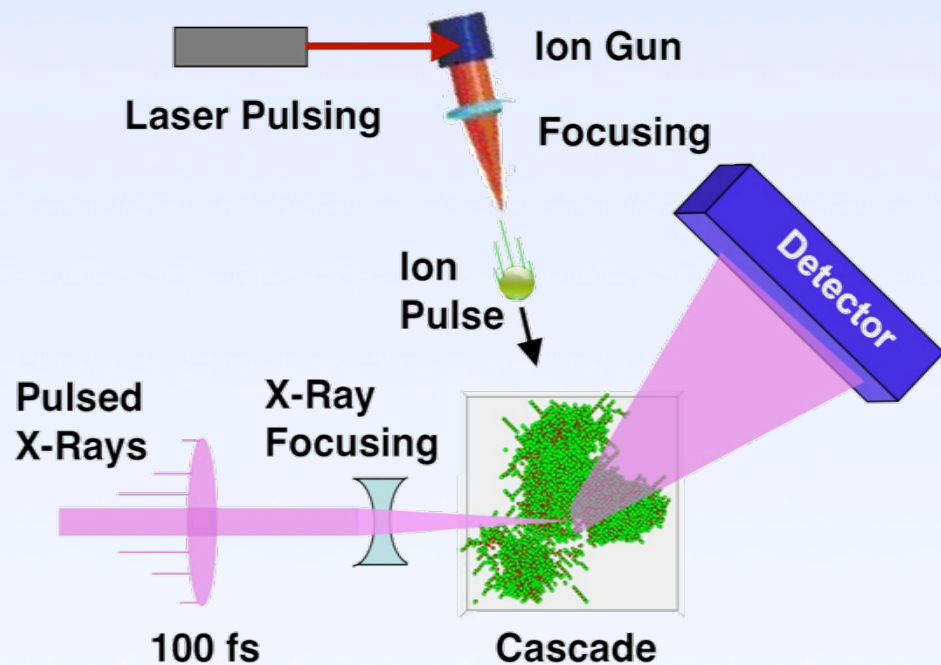
*No Real-Time Measurements of Structural Dynamics !
Impact of Electronic Excitations is Not Included*



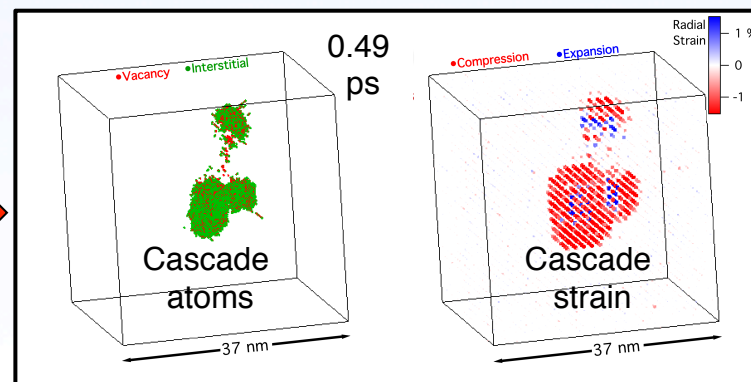
Sub-Picosecond X-Ray Pulses At the Linac Coherent Light Source (LCLS)

First Real-Time Measurements of Cascade Dynamics, and the First Direct Measurement of Electronic vs Ionic Partition

Sub-picosecond Sensitivity of Diffuse Scattering to Cascade Dynamics Using 100-fs LCLS Pulses



300 fs



Concluding Comments

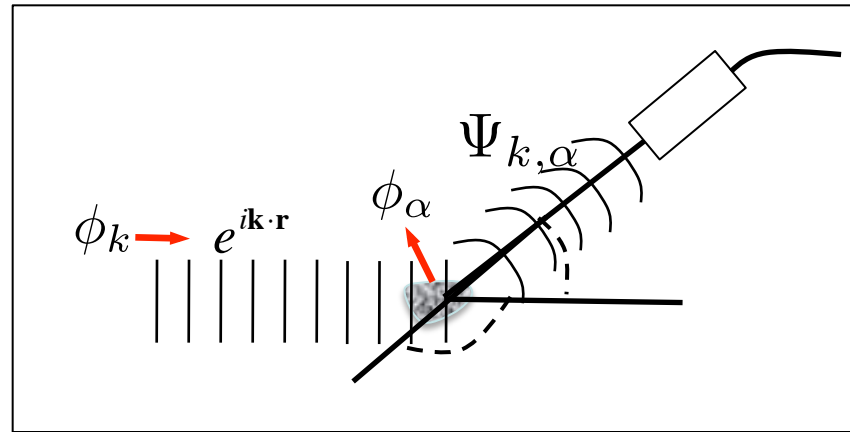
- Radiation environment induced lattice defects have dynamics and evolution on time scales ranging from **femto-seconds to giga-seconds**
- Powerful theoretical frameworks exist for determining **the response of scattering probes** to lattice defects and defect clusters
- Diffuse scattering measurements combined with numerical cross-section calculations provide **detailed information on defect clusters**
- Accurate lattice displacements and strain fields surrounding defect clusters are **critical for extracting defect cluster size distributions**
- Diffuse scattering provides a method for pump-probe investigation of the **dynamics and evolution of displacement cascades on picosecond and longer times scales** using sub-picosecond x-ray pulses at the recently commissioned Linac Coherent Light Source (LCLS)
- Molecular dynamics and kinetic Monte Carlo simulations have not been tested experimentally below milliseconds – **comparisons with time-resolved diffuse scattering will benchmark our understanding of cascade dynamics and defect evolution at early stages within cascade formation and evolution**

Appendix

Supplementary Details and Studies

- Formal theory of scattering
- Theory of the coherent wave
- Huang diffuse scattering closed form expression
- Statement of single defect approximation

Formal Theory of Scattering Solution for Defects



The Lippmann-Schwinger equation provides a formal solution for the scattering of a particle ϕ_k by a crystal in a state ϕ_α with an interaction potential V

$$\Psi_{k,\alpha} = \phi_k \phi_\alpha + \frac{1}{E_k + E_\alpha + i\epsilon - h_o - H_o} V \Psi_{k,\alpha}$$

Particle $\longrightarrow h_o \phi_k = E_k \phi_k$

Crystal $\longrightarrow H_o \phi_\alpha = E_\alpha \phi_\alpha$

$$V(r) = \sum_i v_i(r - r_i)$$

$\phi_k \phi_\alpha \longrightarrow$ Homogeneous solution ($V = 0$)

We need a solution for the scattering from a crystal with an “ensemble” of states (e.g. thermal vibrations, defect clusters)

$$\phi_{Crystal} = \sum_\alpha C_\alpha \phi_\alpha \quad \text{where} \quad C_\alpha = \frac{e^{-\frac{E_\alpha}{kT}}}{\sum_\alpha e^{-\frac{E_\alpha}{kT}}}$$

Coherent Wave Scattering from An Ensemble of States

This problem has been solved elegantly within the theory of the Coherent Wave by Lax* and more recently by Dederichs* through determining that part of the scattered wave $\Psi_{k,\alpha}$ from a crystal with an ensemble of states that is fully coherent with (i.e. interferes with) the incident wave ϕ_k . Performing the interference experiment and averaging $\langle \rangle$ over states:

$$I = \langle |\phi_k + \Psi_{k,\alpha}|^2 \rangle = \langle \phi_k^* \phi_k + \Psi_{k,\alpha}^* \phi_k + \phi_k^* \Psi_{k,\alpha} + \Psi_{k,\alpha}^* \Psi_{k,\alpha} \rangle$$

After (for convenience) adding and subtracting the term $\langle \Psi_{k,\alpha}^* \rangle \langle \Psi_{k,\alpha} \rangle$, we get:

$$I = \phi_k^* \phi_k + \langle \Psi_{k,\alpha} \rangle \phi_k + \phi_k^* \langle \Psi_{k,\alpha} \rangle + \langle \Psi_{k,\alpha}^* \Psi_{k,\alpha} \rangle + \{ \langle \Psi_{k,\alpha}^* \rangle \langle \Psi_{k,\alpha} \rangle - \langle \Psi_{k,\alpha}^* \rangle \langle \Psi_{k,\alpha} \rangle \}$$

where ϕ_k is not affected by the crystal $\langle \rangle$ ensemble averaging. This leads to:

$$I = \phi_k^* \phi_k + \langle \Psi_{k,\alpha} \rangle \phi_k + \phi_k^* \langle \Psi_{k,\alpha} \rangle + \langle \Psi_{k,\alpha}^* \rangle \langle \Psi_{k,\alpha} \rangle + \langle \Psi_{k,\alpha}^* \Psi_{k,\alpha} \rangle - \langle \Psi_{k,\alpha}^* \rangle \langle \Psi_{k,\alpha} \rangle$$

This produces a factor containing $\langle \Psi_{k,\alpha} \rangle$ that interferes with ϕ_k and an additional term that is the well known form of a fluctuation term that is not absolutely coherent with ϕ_k

$$I = |\phi_k + \langle \Psi_{k,\alpha} \rangle|^2 + \langle \Psi_{k,\alpha}^* \Psi_{k,\alpha} \rangle - \langle \Psi_{k,\alpha}^* \rangle \langle \Psi_{k,\alpha} \rangle$$

*M. Lax, Rev. Mod. Phys. **23**, 287 (1951); P.H. Dederichs, Solid State Physics 27,135 (1972).

Calculation of the Huang Scattering Term Using the Dipole Force Tensor*

The dipole-force tensor with the Fourier transformed elastic Green function provide a closed form expression for the so-called Huang scattering amplitude

$$|\vec{h} \cdot \vec{s}(\vec{q})|^2 = |(h_i/V_c)G_{in}P_{nm}q_m|^2. \quad (4)$$

Summation over repeated indices is assumed and

$$G_{in} = \frac{1}{q^2} \left\{ \frac{\delta_{in}}{C_{44} + de_n^2} - \frac{e_i e_n}{(C_{44} + de_i^2)(C_{44} + de_n^2)} \right. \\ \left. \times (C_{44} + C_{12}) / \left[1 + \sum_k \left(\frac{C_{44} + C_{12}}{C_{44} + de_k^2} \right) e_k^2 \right] \right\}, \quad (5)$$

where $e_i = q_i / |\vec{q}|$, $d = C_{11} - C_{12} - 2C_{44}$, and the C 's are the elastic constants. The dipole-force tensor of a spherical defect cluster is isotropic⁴ and is given in terms of the strength P_0 of the cluster by

$$P_{nm} = P_0 \delta_{nm}. \quad (6)$$

For dislocation loops³ the force tensor is

$$P_{nm} = (C_{12} \text{Tr} \Omega_{nm} + d \Omega_{nm}) \delta_{nm} + 2C_{44} \Omega_{nm}, \quad (7)$$

where [not to be confused with $(\Delta\Omega)_D$ in Eq. (1)]

$$\Omega_{nm} = \frac{1}{2}(F_n b_m + F_m b_n), \quad (8)$$

$$\langle |\vec{h} \cdot \vec{s}(\vec{q})|^2 \rangle = \left(\frac{h}{q} \right)^2 \sum_{i=1}^3 \gamma_i \pi_i, \quad (9)$$

where $\langle \rangle$ denotes the average over cubic-equivalent orientations and

$$\gamma_1 = \frac{1}{3}(\text{Tr} T_{ij})^2, \\ \gamma_2 = \frac{1}{3} \sum_{i>j} (T_{ii} - T_{jj})^2, \\ \gamma_3 = \frac{1}{2} \sum_{i>j} (T_{ij} + T_{ji})^2, \quad (10)$$

and where

$$T_{ij} = (\hat{h}_k / V_c) g_{ki} e_j \quad (11)$$

with $\hat{h}_k = h_k / |\vec{h}|$ and $g_{ki} = q^2 G_{ki}$. Similarly,

$$\pi_1 = \frac{1}{3}(\text{Tr} P_{nm})^2, \\ \pi_2 = \frac{1}{6} \sum_{n>m} (P_{nn} - P_{mm})^2, \\ \pi_3 = \frac{2}{3} \sum_{n>m} P_{nm}^2, \quad (12)$$

*B.C. Larson and W. Schmatz, Phys. Stat. Sol. (b), **99**, 267 (1980)
P.H.Dederichs, J. Phys. F: Metal Phys., **3**, 471 (1973)
P.H.Dederichs, Phys.Rev. B4,1041 (1971)

Separation of Bragg and Defect Diffuse Scattering

For the kinematic case the total scattering is given by:

$$\frac{d\sigma(\mathbf{K})}{d\Omega} = |r_e f(\mathbf{K})|^2 |A(\mathbf{K})|^2 = \left| \sum_i r_e f_i(\mathbf{K}) e^{i\mathbf{K}\cdot\mathbf{r}_i} \right|^2$$

For r_i = perfect lattice sites \rightarrow Bragg Scattering

For r_i = distorted lattice sites \rightarrow Fluctuation or Diffuse Scattering

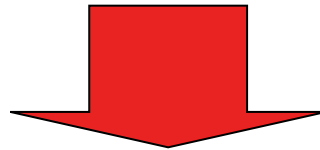
$$\left[\frac{d\sigma(\mathbf{K})}{d\Omega} \right]_{Diffuse} = \left[\frac{d\sigma(\mathbf{K})}{d\Omega} \right]_{Total} - \left[\frac{d\sigma(\mathbf{K})}{d\Omega} \right]_{Bragg}$$

Single Defect Approximation for Diffuse Scattering

For randomly distributed defects (or clusters) with static Debye-Waller factor given by,*

$$L(\mathbf{K}) = c \sum_i [1 - \cos(\mathbf{K} \cdot \mathbf{s}(\mathbf{r}_i))] \approx c \sum_i \frac{(\mathbf{K} \cdot \mathbf{s}(\mathbf{r}_i))^2}{2}$$

The diffuse scattering in the so-called “**Single Defect Approximation**” results is given by,



$$\left[\frac{d\sigma(\mathbf{K})}{d\Omega} \right]_{Diffuse} = \left| \sum_j^{n^d} r_e f_j^d e^{i\mathbf{H} \cdot \mathbf{r}_j^d} e^{i\mathbf{q} \cdot \mathbf{r}_j^d} + \sum_i r_e f_i e^{-L(\mathbf{K})} e^{i\mathbf{q} \cdot \mathbf{r}_i} \left[e^{i\mathbf{K} \cdot \mathbf{s}(\mathbf{r}_i)} - 1 \right] \right|^2$$

Sum over atoms in defect cluster
Sum over atoms in distorted lattice surrounding cluster

This is a fundamental result discussed in more detail by Dederichs